UNIVERSITY OF TARTU

FACULTY OF SCIENCE AND TECHNOLOGY

Electron- vibrational coupling in phycobiliproteins of Acaryochloris marina

MASTER THESIS

Galyna Gryliuk

Supervisor: Prof. Jörg Pieper

TARTU 2013

Contents

1. List of abbreviations

A.marina – Acaryochloris marina

APC – allophycocyanin

Chl – chlorophyll

Chl d' – minor pigment

CIP – color intensity plot

DAS –decay associated spectra

EET – excitation energy transfer

FLN – difference fluorescence line narrowing

FWHM – full width

IDF – inhomogeneous distribution function

PBP – phycobiliproteins

PBS – phycobilisomes

PC – phycocyanin

Pcb – prochloropyte chrolophyll binding proteins

PE – phycoeretrin

PSB – phonon sideband

RC – reaction center

SHB –spectral –hole burning

TRS –time resolved fluorescence spectra

ZPH –zero – phonon hole

ZPL –zero phonon line

2. Introduction

Photosynthesis is one of the most important processes on earth on which depends the existence of human and almost all other living organisms. It is the process by which plants convert light energy into chemical energy in the form of different organic compounds and sugar. This process occurs in algae, plants and some prokaryotes.

During evolution nature has developed highly specialized specialized antenna pigment-protein complexes for efficient light harvesting and excitation energy transfer (EET) to reaction center (RC) complexes. There primary charge separation and secondary electron transfer occur [1].

The cyanobacterium *Acaryochloris marina* (*A.marina*) contains Chlorophyll (Chl) *d* as the dominant photosynthetic pigment which is different from other oxygenic photosynthetic organisms [2]. A. marina lives under a sea squirt so that containing a thick layer of Chl a/b. It gives *A. marina* opportunity to exploit far red light above 700 nm in habitats with largely reduced visible light. [2, 3]

The antenna system of *A.marina* includes the membrane external phycobiliproteins (PBP), the core light-harvesting complexes CP43/CP47 [5] and the membrane internal Prochlorophyte Chl *d* binding Pcb (prochloropyte chlorophyll binding) proteins [4].

Up to now, *A.marina* has mainly been studied by time-resolved spectroscopy [7]. Some preliminary studies on PBP of *A.marina* using site selective spectroscopy were done (for reviews see [6, 8]), but these studies were not too detailed. To get better understanding of EET in PBP of *A.marina*, the results of time-resolved spectroscopy have to be supplemented by investigations of spectral positions and excitonic nature of excited electronic states and of electron-vibrational coupling. But because of the amorphous nature of pigment-protein complexes, such spectral substructures are hidden by serious inhomogeneous broadening even at low temperature circumvent. SHB and delta-FLN are proper techniques to circumvent inhomogeneous broadening and to obtain information on homogeneously broaden spectra [6].

Therefore, the aim of this thesis is to obtain parameters of homogeneously broadened spectra using site-selective spectroscopies like difference fluorescence line - narrowing (ΔFLN) and spectral hole - burning (SHB). The present study is based on application of SHB and ΔFLN spectroscopy for an investigation of excited state positions as well as homogeneous and inhomogeneous broadening of PBP.The results obtained provide valuable information for a further understanding of EET in the PBP antenna of *A. marina*.

3. Literature overview

3.1. Photosynthesis

Photosynthesis is a process by which green plants, algae and bacteria transform light energy into chemical energy. During this process is converted into organic material by reducing the gas to carbohydrates in a multiple number of reactions. Electrons which come from water cause the reduction reaction, which is eventually converted into protons and oxygen. There are few types of pigments that the light energy is absorbed by for photosynthesis. These pigments include chlorophylls, carotenoids and phycobilins. Chl *a* and Chl *b* are two pigments which predominate in plants. Their molecular structure has only a slight differ. On (Fig.1) is showed that the chlorophylls absorb blue and red wavelengths, that are close to the ends of visible spectrum.

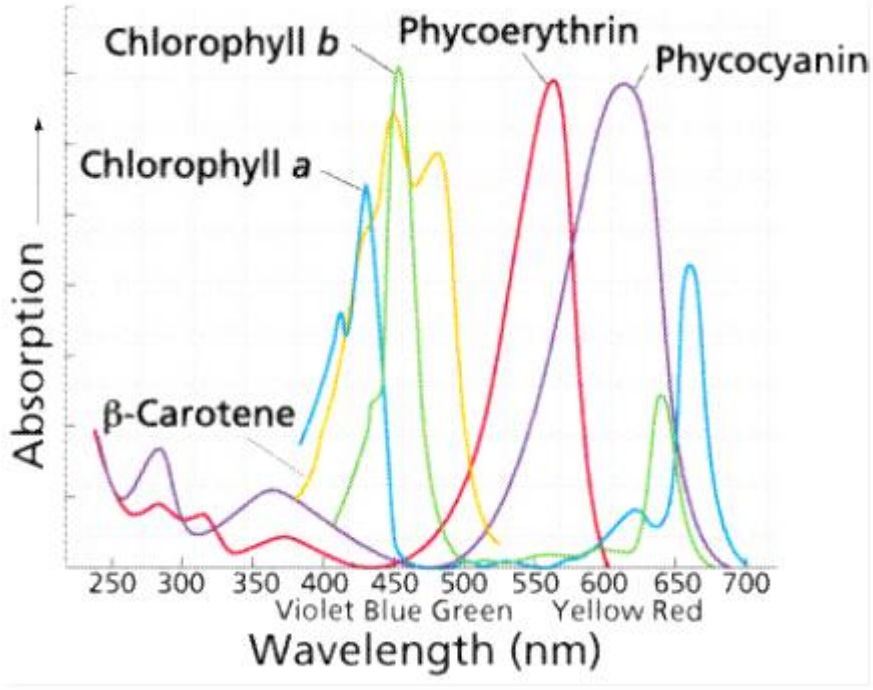

Figure 1. Absorption spectrum of different pigments. The color shows the various of wavelengths which are indicated above the graph (according to [9])

As the latter spectrum shows photosynthetic pigments in plants do not efficiently absorb green and yellow light, because this light passes through leaves or reflected by leaves. This is the reason why plants have a green color. However, all photosynthetic organisms possess accessory pigments. They absorb photons intermediate in energy between the blue and red wavelengths and then transfer a part of that energy to chlorophylls. These accessory pigments are carotenoids, for

example -carotene. They absorb photons in the blue and blue – green wavelength and appear yellow color. Some photosynthetic organisms like cyanobacteria and red algae have additional pigments named as phycocyanobilins. They absorb various yellow – green, yellow and orange wavelengths. So accessory pigments, in co-operation with chlorophylls, compose an energy – absorbing system covering much of the visible spectrum [10].

Cyanobacteria essentially absorb solar energy in the visible spectral (400-700) re-gion by use of clorophylls. Bacterias which are anoxygenic phototrops absorb infrared wavelengths (> 700 – 1100 nm) by bacteriochlorophylls. All groups have a variety of characteristic antenna pigments and also accessory pigments which increase light capture or provide protection against UV-radiation in specific habitats and excess actinic light [10, 11].

3.2. Discovery of Chl *d* and *A. marina*

Firstly Chl *d* was found in pigment extract from red algae. The difference in chemical structure between Chl *d* and Chl *a* is just a presence of a 3-formyl group, which replaces the vinyl group on ring 1 in Chl *a* (Fig. 2).

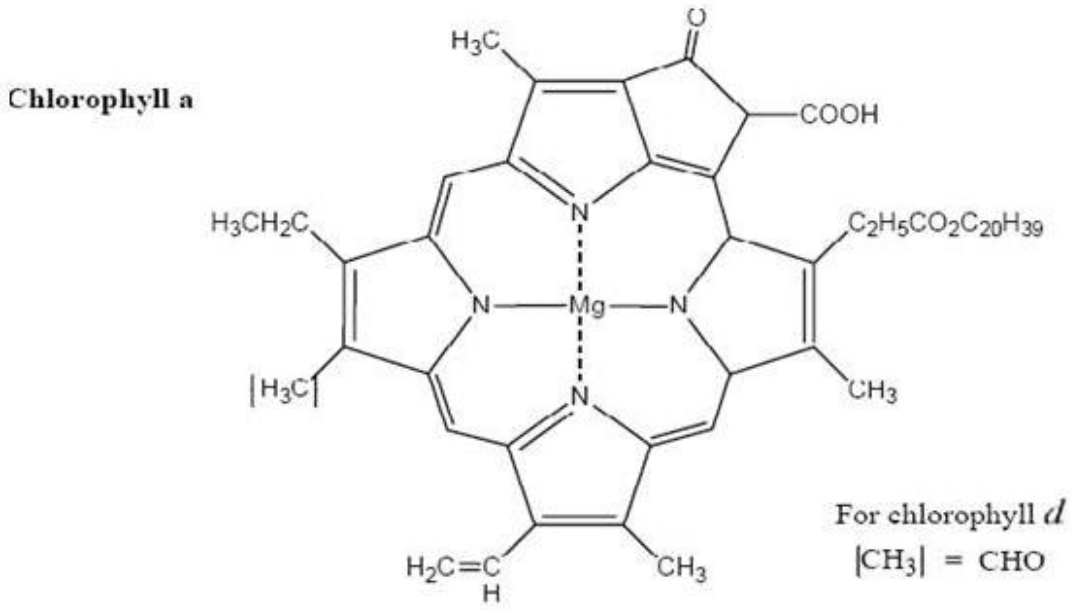

Figure 2. Molecule structure of Chl *a*, where is shown the difference with Chl *d*.

The reason of structural changes is the Qy absorbtion maximum of Chl *d* which has red shift by about 30 nm comparing to Chl *a* (Fig. 3). The region of cell absorption of *A. marina* is at 710-720 nm [11].

A. marina was discovered in 1996 and it possessed mainly Chl *d*, small amount of Chl *a* and phycobiliproteins. Many questions concerning the role of this Chl have been raised from the discovery of organisms where Chl *d* is the predominant pigment. The new chlorophyll could not be considered as a new specific organism and it was proved that Chl *d* could also be formed as an intermediate byproduct from other chlorophylls during pigment extraction [11, 13].

Before *A. marina* was discovered it was assumed that all primary electron donors in oxygenic photosynthesis were in essence Chl *a* molecules. Nowadays it was proved that the reaction center of PSI in A. marina uses a special pair of Chl *d*, which has a name P740 [12, 13].

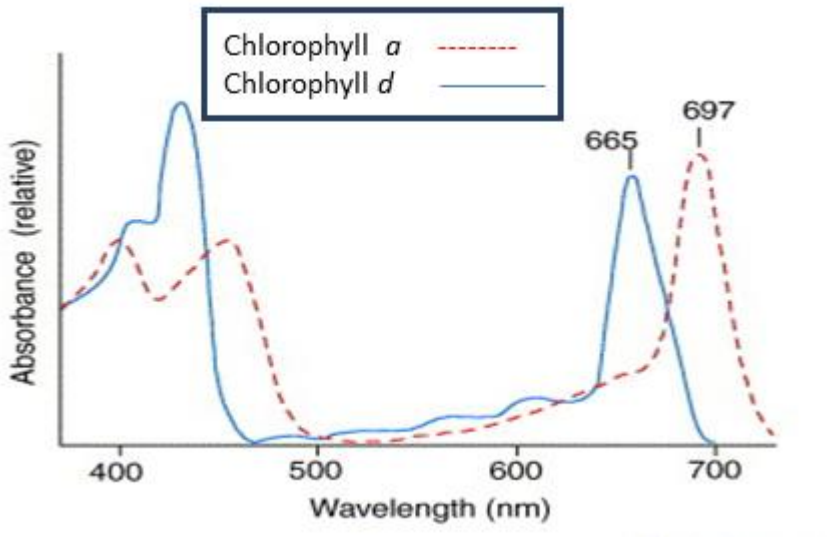

Figure 3.Spectrum which shows the Qy absorption maximum of Chl *d* which has about 30 nm shift in comparison with Chl *a*. (according to [3]).

3.3. Cell Biology of A. marina

A. marina has ellipsoidal shape, 1,8 – 2,1 × 1,5-1,7 μm in size and it is unicellular non-motile cyanobacterium. It has about 6-12 layers of thylakoid membranes which are arranged peripherally in the cells. If to compare it with other cyanobacteria it doesn't have phycobilisomes [11].

Excitation states of Chl *d* and Chl *a* are different, Chl *d* has lower energy than Chl *a*. As *A. marina* has a low content of Chl *a*, such question as composition of the RCs and mechanic of EET have arised [14]. The PS I RC complex of *A.marina* employs Chl *d* both as the primary electron donor P 740 and the major antenna pigment. If we compare *A. marina* PS I with cyanobacterial PS I we can see the effects of employing different Chls in the PS I RC complexes that are made up of highly homogeneous Psa A /Psa B polypeptides [15]. This will show the evolution of oxygenic

photosynthesis from more primitive anoxygenic one that uses bacteriochlorophylls with absorbance near infrared light of 800 - 900 nm [18].

For instance, PS I of *A. marina* , which is the primary donor of the RC was displayed to be a heterodimer consisting of Chl *d* and Chl , a pimer of Chl *d* [6], that was before shown to absorb at 740 nm and that's why named P740 [17]. Intact cells of *A. marina* have such pigment composition: two pheophytin *a*, two Chl explain per 140 Chl *d*, and four Chl *a*. Isolated PS I complex of *A. marina* has 145 ±8 Chl *d* and only a trace amount of Chl *a* were obtained per P740 [15]. There is no precise data about PS II till nowadays. It was indicated that Chl *d* works as the major pigment molecule both in PS I and PS II, this information was obtained using the fluorescence properties of intact cell of *A. marina*. Also it was thought that PS II has a special pair of Chl *a* - like pigment. Trusted results of chemical identity of the electron donor pigment in PS II have not been obtained yet [18].

3.4. Structure comparison of A. marina and other Chl *a* containing cyanobacteria

A.marina in addition to the CP43/CP47 light harvesting proteins of PS II core complex has a membrane internal Pcb protein complex which binds Chl *d* and it has a similar structure as CP43. This is one of the differences to other Chl *a* containing cyanobacteria. The coming together of 16 Pcb complexes with two PS II – RC core dimers is a great complex which increases the efficiency of harvesting the light of the PS II core complex by almost 200 % [14].

It was noticed that very often Pcb light harvesting complexes are found in a group of cyanobacteria lacking PBPs where they bind both, Chl *a* and Chl *b*. For comparison, strain MBIC 11017 of *A.marina* has membrane internal Pcb complexes and a membrane external PBP - light harvesting antenna with absorption band around 618 nm. It makes possible the utilization of visible light by strain in a "green gap" between 500 nm and 650 nm where the chlorophylls have limited absorption capabilities [14].

The EET in *A. marina* is combined as shown in Fig.4 (left panel). In this picture, it is taken to be that the PBP antenna of *A.marina* compares the rods of the phycobilisomes in other cyanobacteria with the main distinction that a heterohexamer consisting of one PC- and one APC-trimer is the hexamer closest to the thylakoid membrane [21]. The Synechococcus 6301 was taken as an example and shown in fig. 4, right panel. There are four kinetic components with lifetimes o< 400 fs, 3ps, 14 ps and 70 ps, which describe the EET from PC to Chl d [14].

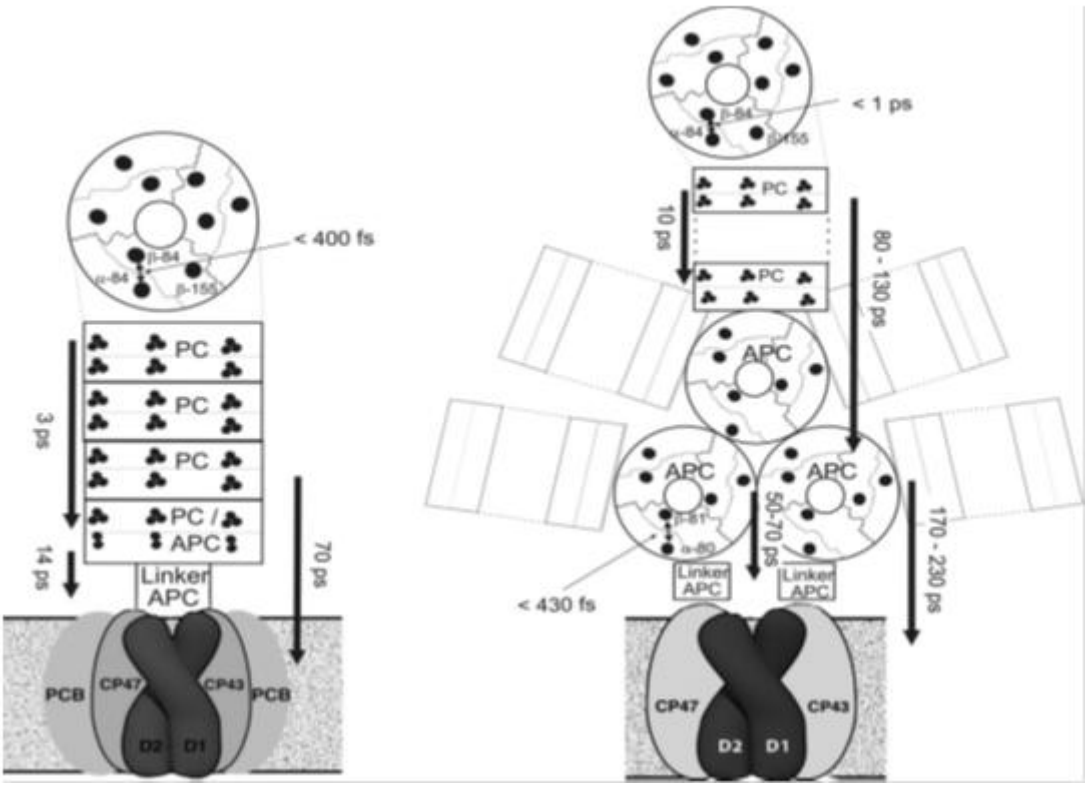

Figure 4. Scheme of excitation energy transfer (EET) processes in A. marina and in the cyanobacterium Synechococcus 6301. (Left panel) EET inside the PBP antenna rod of A. marina and overall EET to the reaction center of PS II. At the top a scheme of the PC trimer with its bilin chromophores is shown. (Right panel) EET inside the the phycobilisomes of Synechococcus 6301 giving a resume of data reported in the literature [19, 20]

Fig. 4 (right panel) describes a scheme with the range of time constants for EET processes in Synechoccus 6301, where the equilibration along the trimetric PC disks in the PC containing rod displays with a typical rate of about [19]. A random walk model for the EET in the PC rods of Synechoccus 6301 was presented using the experimental results from ps – studies [20]. Also rates of and for single step EET between trimeric PC disks and about to for the EET from the inmost PC trimer to the APC core were calculated. For the general EET from a PC rod containing 4 hexamers to the APC core the literature findings rate constants of to [22] (see Fig. 4 (right panel)).

In a comparison with A. marina where APC and PC share the same hexamer, the PC to APC EET happens with a rate constant of only and this is around 8 times faster than the EET rate from the innermost PC trimer to the APC core in phycobilisomes as given in [23] (Fig. 4 (left panel)). Also it is faster than the single step EET between neighboring trimers in pure PC rods of another type of cyanobacteria. [14].

The unique feature of a compact single rod shaped PBP antenna is caused by a very fast EET in *A. marina* from PC to APC then to CHL *d.* In this antenna PC and APC share the same heteroxamer instead of a very big phycobilisomes with rods containing PC only and an additional APC core [14].

Structure scheme of the PS II antenna system of *A.marina* is shown on figure 5 (right). The photosynthesis takes place in staples of the thylakoid membrane, which is included in the prokaryotic cells of *A. marina*. The membrane extrinsic antenna is represented by a PBP rod which is associated to the PS II core antenna containing Chl *d* [24].

The structure of the phycobilisomes (PBS) of *A.marina* comprises aggregates which is simpler than the one in the typical cyanobacteria. It has four hexameric units, which resemble the peripheral rods of the typical cyanobacterial PBS. Three hexamers contain only one phycocyanin (PC) and the fourth hetero - hexamer containing PC and allophycocyanin (APC). The structure of these rods can be different depending on the species. The excitation energy seems to be funneled directly from the APC – containing hetero - hexamer to Chl *d* of PS II without the involvement of an APC core as in typical cyanobacteria. Isolated PBP aggregates of *A. marina* have a pronounced fluorescence maximum at 665 nm which caused by APC and a shoulder at about 655 nm, produced from PC at room temperature [24].

There is no certain information about the PBP link with the photosystem-reaction center in *A. marina*. After the analysis based on the action spectra of intact cells of *A. marina* was obtained that the PBPs transfer energy to PSII has higher efficiency than to PSI. Some excitation energy transfer studies with time-resolved fluorescence spectroscopy were carried out. It was indicated that the elemental structure of PBP in *A. marina* provides efficient energy transfer from PBP to Chl *d* in PSII with a time constant of 70 p. It is three times faster than energy transfer in comparison with phycobilisomes to PSII in the Chl *a* - containing cyanobacteria [11].

In comparison with *A. marina* the PBP are organized in the form of phycobilisomes in other cyanobacteria (Figure 5 right). They are complex, which consist of colorless linker polypeptides and highly structured assemblies of phycobiliproteins that have a bright color.

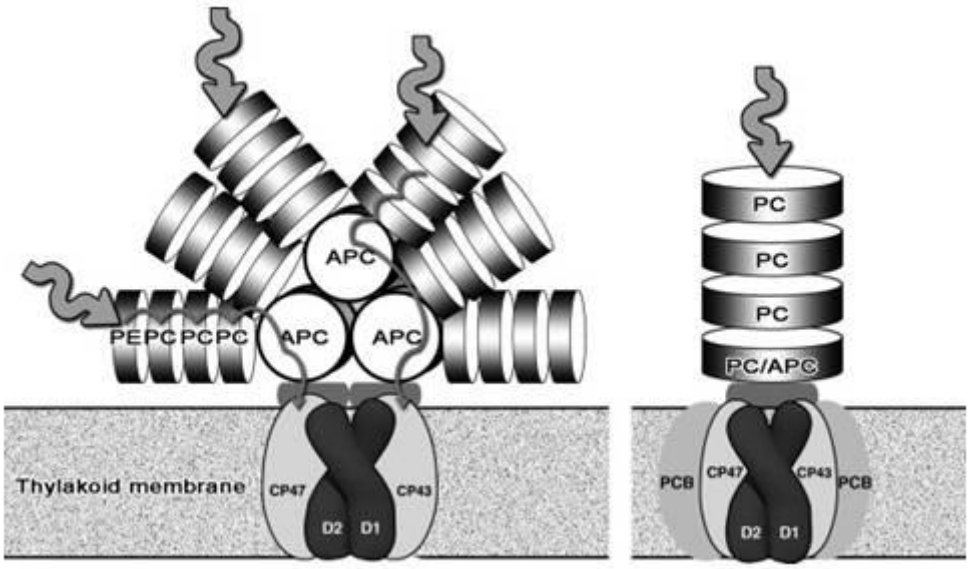

Figure 5. Structure of a tri – cylindrical hemidiscoidal phycobilisome in "typical" cyanobacteria (left side) and of rod shaped phycobiliprotein light harvesting complex and of PS II in *A. marina* according to [4, 21] (right side).

Phycobilisomes are composed of predominantly hydrophilic polypeptides in comparison to most other light- harvesting antennae. Hydrophilic polypeptides located in cytoplasm and associated with the cytoplasmic surface of the thylakoid membrane [25].

It has a core complex that includes allophycocyanin (APC) and often six rods type structures radiating from the core complex. The rods are made up of stacked discs. The discs which are close to core contain PC, when discs distal to the core contain PE (phycoeretrin). There is a difference between the main absorption bands: PE (560-575 nm), PC (618 nm), APC (652 nm) [14, 26].

3.5. Energy transfer aspects of the phycobilisomes

The PBS have such molecular architecture where the excitation energy absorbed by the same phycobiliproteins is transferred to the PS II reaction center. The efficiency of transfer is around 80-90% [26].

Some research studies of the sequential energy transfer in higher plant Chl antenna were done by Porter's group using pico second time-resolved spectroscopy. The studies were done using direct measurement and previous proposed sequential energy transfer research was confirmed. The research work were done by [27] in using picosecond time-resolved energy transfer method. These studies proved the fact that the energy transfer occurs from PE to PC to APC [26]. The data received by using the time-resolved fluorescence and absorption spectroscopy helping to prove the

idea of an arrangement of chromophores ordered within the PBS. Several structural features make the directional energy transfer in PBS possible [26]:

1) There is *s* and *f* (sensitizing and fluorescing) chromophores in each type of the biliproteins .The *f* chromophores of PE plays role of sensitizers in the transfer of excitation energy to PC in PE-PC PBS or hetero aggregates. Transfer occurs more often between hetero aggregates than among homo aggregates. It was made an assumption that the transfer of excitation energy from one disc to new disc within the PBS rod is rate limiting step in PBS [26].

2) There are six separate domains in the rod sub-structure of PBS, the inter-rod transfer of energy is prohibited by distance constraints [26].

3) Transfer within the rod has directional type. The minimization of reverse energy transfer happens due to energy difference between different rod elements and the core. Also this phenomenon allows the long wavelength absorbing core to serve as efficient traps. The molecular architecture of PBS which was mentioned above showed ensures the minimization of random walking and the existence of the directional energy transfer to the final emitter in the core of the PBS [26].

There are few environmental factors which affect the energy transfer (phycocyanin to chlorophyll a) in cyanobacteria:

1) Enormous variations in the pigmentation of cyanobacteria, which result from different illumination conditions. They are known as complementary chromatic adaptation.

2) Due the presence of only PC in the PBS rods, cells which were grown in red light appear to be blue green in colour. Brown pigmentation indicates the presence of both PE and PC, it can happen if these cells are transferred to green or cool white fluorescent light. Different environmental factors which were mentioned help to affect the efficiency of energy transfer from pc to Chl *a* by affecting the pigment protein interaction i.e nitrogen stress, heat treatment, mercury stress and low temperature [26].

3.6. Excitation energy transfer in cells of A. marina

The information about electron transfer in living photosynthetic species and EET can be achieved by using non – invasive techniques of time-resolved optical spectroscopy which obtain high quality signal – to – noise ratios at low excitation light intensities. The results received by using isolated complexes of the PBP antenna of *A. marina* have to be compared with the spectroscopic measurements of whole cells. In this case it can be shown that the preparation process did not change the molecular configuration of the PBP. Samples for spectral hole – burning and transient absorption spectroscopy with *fs* time resolution should have good optical quality and

cannot be done on living cells. For investigation of EET processes directly in living cells of *A. marina* was used the additional technique of wavelength- and time-resolved single photon counting fluorescence spectroscopy. Usage of this technique helps to obtain high quality signals at a time resolution of about 20 ps. *A. marina* is an ideal model organism to study EET processes with fluorescence spectroscopy because there is a huge energetic difference between the excited states of Chl *d* and the PBP antenna [14, 24].

Fig. 6 describes fluorescence measurement of whole cells of *A.marina* upon excitation at 632 nm. A two – dimensional data matrix was used as a storage of the registered photons at each time channel and wavelength. Fig. 6*a* shows a color intensity plot (CIP) which was obtained by using the data matrix and shows the fluorescence intensity. The information about time – resolved fluorescence spectra and the dynamics of different emitter states can be obtained from the CIP [14, 24].

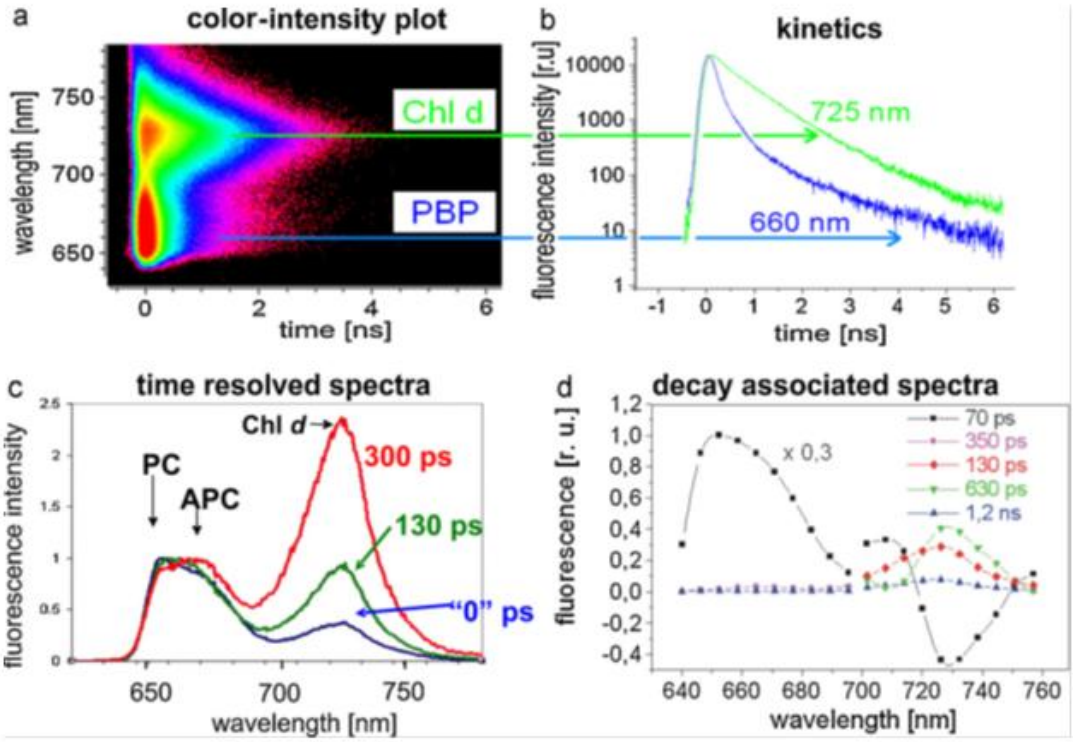

Figure 6. Fluorescence dynamics in whole cells of A. marina at 25 ◦C upon excitation at 632 nm (according to Petrasek et al., 2005). (a) Color intensity plot (CIP) of time- and wavelength resolved fluorescence matrix F(t,) of the experimental data; (b) normalized fluorescence decays at 660 nm and 725 nm; (c) time resolved fluorescence spectra (TRS) at "0" ps, 130 ps and 300 ps after excitation (the TRS are normalized to 1 in the PBP emission band for better visibility); (d) decay associated spectra (DAS) of a global fit of the data with three exponential decay components in the 640–690 nm range (scaled by a factor 0.3) and a global fit with four exponential decay components in the 700–760 nm range. The fluorescence below 645 nm is cut off by a long-pass filter from [14]

In fig. 6 *c* showed fluorescence spectrum called time resolved spectra because it has different time intervals. It shows the fluorescence of certain fluorophores at later times. It happens when scattered light or the fluorescence emission of other pigments already decayed. Fig. 6 *b* allows seeing that the Chl *d* emission at 725 nm decays much slower than the PBP - fluorescence at 660 nm. It was made a multi – exponential decay model using eq. (1) in which ten decays at were fitted together, each of decay had a different wavelength.

(1)

In fig. 6 *d* described decay associated spectra (DAS). Individual decay components have different energetic position which is shown by DAS. The fits of few decay graphs which are fitted together have a name of a global fit [14, 26].

After the research results reported [28] was compared with [29]. Conclusively the life times results of the 725nm fluorescence band achieved by Mimuro are greatly consistent with those obtained by Theiss. The results of [13] showed a higher relative contribution of the slow component, ns about 25% at room temperature in comparison with ≤ 5 % obtained by Mimuro. This difference might happen because of huge fraction of closed RCs in the measurements results in [14].

In the TRS of Fig. 6 *c* is also shown the EET from PC to Chl *d* via APC. After excitation (“0” ps) the dominant fluorescence is observed at 650 nm. PBP emission has the emission peak which is shifted from 650 nm in PC emission to 670 nm in APC emission [14].

3.7. Fluorescence line narrowing and hole burning spectroscopies

The results obtained by time-resolved spectroscopy have to be supplemented by research of excitonic nature of excited electronic states of electron - vibrational coupling in the frequency domain and spectral positions. These spectral substructures are hidden by inhomogeneous broadening which is a result of the amorphous nature of pigment - protein complexes. It shows that fluorescence measurements and the resolution of conventional absorption have limitation to the inhomogeneous width of the excited states in practice. From the other point of view, inhomogeneous broadening can be rationally outwitted by using difference fluorescence line – narrowing at low temperatures and spectral hole - burning which are site – selective spectroscopy methods [14].

The pigments absorbing at individual frequencies within inhmogeneously broadened spectra are selected by quasi – monochromatic laser light, which is used in site – selective spectroscopy

methods. In this case the results can be related to their homogeneously broadened spectra. This method will be described for the case of PBP dissolved in a buffer solution containing 70% glycerol [14, 30].

Fig.7 shows the 4,5 K absorption spectrum of PBP (black upper line labeled as I and II). This spectrum is widely features even if it has low temperature and has only two peaks at and . There are two peaks at and 644 nm on the 4,5 K fluorescence spectrum (labeled as III and IV in fig.7). The line-narrowing effect on the 637 nm cannot be ruled out, because the excitation wavelength of 631 nm is located in the main absorption band at 629nm and in the range of the blue edge of the inhomogeneously broadened fluorescence maximum [14].

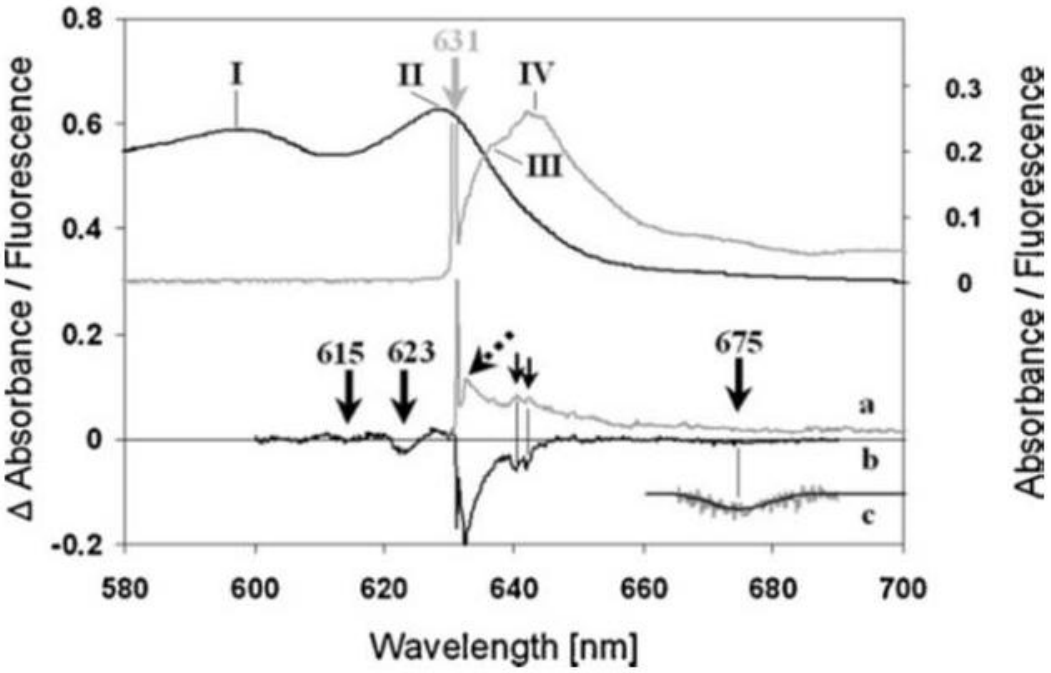

Figure 7. Upper part (right scale): 4.5 K absorption (black line) and fluorescence (grey line) spectra of PBP in a buffer solution containing 70% glycerol. The fluorescence spectrum was excited at 631 nm. The narrow line at 631 nm in the fluorescence spectrum is contaminated with scattered excitation laser light and thus cut off at 25% of its full intensity. The peaks observed in these spectra are labeled by I–IV. Lower part (left scale): Site selective hole-burning (black line – curve b) and difference fluorescence line-narrowing (grey line – curve a) spectra burned/excited at 631 nm. The burn/excitation wavelength is indicated by a full grey arrow, satellite holes are labeled by thick black arrows and their peak wavelength. Curve c is a magnification of the 675 nm satellite hole region of curve b, which is fitted by a Gaussian with a full width (FWHM) of 220 cm−1 (according to [30]).

Detailed spectral substructure was investigated by SHB at the burn wavelength of 631 nm. Lower part of fig. 7 shows SHB spectrums (black line). This figure can be divided into four main features:

I. A narrow hole congruous with the burn wavelength ;

II. PSB located to the red of the narrow hole;

III. Shallow and Broad hole at

IV. Two consecutive holes at and

The hole features with the burn wavelength of 631 mn principally describe the higher – energy emitting state responsible for the 637 nm band in fluorescence. Presence of a narrow line shows that the absorption band at 629 mn is principally inhomogeneously broadened. Pseudo phonon sideband (PSB) appears from coupling of the electronic transitions to protein vibrations and has frequency of . The real PSB is much weaker and located to the blue of the narrow hole. The grey line in the lower part of fig. 7 is a FLN spectrum excited at 631 nm. There is a huge Stokes - shift around 8 nm supporting the assignment of the 637 nm fluorescence peak to the absorption band at 629 nm, which is caused by strong electron – phonon coupling [14].

The third feature in the SHB described by a shallow and broad hole at , shifted to the red of second main fluorescence band. This notice shows that there is some EET to an electronic state at this position, while main part of fluorescence originates from the excitonic states connected to the fluorescence bands at 637 and 644 nm. [14].

The terminal states of different subunits can be perceived at the same time because of a partial dissection of the PBP subunits in glycerol –buffer and this effect can be seen as advantage. The terminal low – energy states of PC and APC contain the two fluorescence bands at 637 nm and 644 nm seen in PBP in 70 % glycerol at 4, 2 K. Absorption maximum of trimetric APC of A. marina at 642 nm given by [31] is in a very good agreement with 644nm band result, obtained by [30]. The shallow low – energy hole at 675 nm has two possible places of location: in the linker protein or on a pigment in APC so this discovery has to be situated in the terminal state of intact PBP [14].

It was done some research of a doublet of satellite holes to the blue of the burn wavelength of 631 nm. These later holes at 615 and 623 nm appear very intense and shifted very far from the burn wavelength to place to vibronic features. There is a possibility that these holes represent excitonic wave function of two or more interacting molecules [32, 14].

4. Materials and Experimental methods

4.1. Sample Preparation

Cells of A. marina for sample preparation were grown in artificial sea water. These cells containing iron at a concentration of 4 mg/L at 6 – 10 as described in ref. 34. Thylakoid membranes of cells were isolated as reported in ref. 35. PBP were isolated by sucrose density gradient fraction of the detergent solubilized (1% n-dodecyl- - D-maltoside for 45 min at C) thylakoid membranes as shown in ref.34. At the end, the samples were dissolved in a glass- forming buffer solution containing 70 % glycerol [30]. The PBP samples used in the present study were provided by Dr. Hann-Jörg Eckert, Sabine Kussin and Monika Wess (TU Berlin, Germany).

4.2. Experimental setup

The setup for hole burning and fluorescence line – narrowing has been reported in ref. 36. The burn laser at 631 was used a Spectra Physics model 375 dye with a linewidth of <0,5 cm^{-1} pumped by an Ar ion laser (Model 171, Spectra Physics, USA). Transmission measurements employed a 0,3 m spectrograph (Shamrock SR-303i, Andor Technology, UK) and a high stability tungsten light source BPS100 (BWTek, USA). The data were recorded with an electrically cooled CCD camera (DV420A-OE, Andor Technology, UK) operated at a resolution of 0,4 nm. A He-bath cryostat (Utreks, Ukraine) was used to control the sample temperature [30]. The delta-FLN measurements presented in this study were carried out by Dr. Margus Rätsep (FI Tartu, Estonia).

4.3. Data Analysis

The DFLN spectrum in the short burn time limit is widely identical to the homogeneously broadened fluorescence spectrum [33]. For several phonon modes (k) one-phonon profiles and arbitrary temperature this spectrum takes the form [34]

$$L(w) = e^{-\sum_k S_k(2\bar{n}_k+1)} \prod_k \sum_{R=0}^{R} \sum_{r=0} \frac{\left[S_k(\bar{n}_k+1)\right]^{R-r}\left[S_k\bar{n}_k\right]^r}{(R-r)!r!} \, l_{R,r}\left(w - w_0 - \sum_k (R-2r)w_k\right) \quad (1)$$

where $\bar{n}_k = \left[\exp(\hbar w_k / kT) - 1\right]^{-1}$ describes the thermal occupation for phonons of mode k according to Bose statistics and - and + correspond to absorption and fluorescence. Also, R (with

R=1,2,...) denotes the total number of phonon transitions, when r gives the number of annihilated phonons ($0 \leq r \leq R$). The profile $l_{R,r}$ (R>1) is received by folding the one-phonon profile $l_{1,0}$ |R-2r|-times with itself. In this method we employ a one-phonon profile composed of a Gaussian and a Lorentzian shape at its low- and high-energy wings [30].

4.4. Homogeneously broadened spectra

To get a quantitative description of electron – phonon coupling requires a number of simplifying assumptions to be made about the complex macromolecular pigment – protein system, including adiabatic, harmonic and Franck –Condon approximations [35].

The motions of the heavy nuclei of a macromolecule supposed to be uncorrelated with the faster motions of the much lighter electrons so that the two types of motions can be separated. This phenomenon is described by the adiabatic approach. The spectrum of an isolated pigment molecule consists of a narrow purely electronic ZPL (zero phonon line) and a broad PSB lying towards higher energy in absorption (see red line in Frame A of Fig.8). Pigment molecule electronic transition is coupled to a distribution of delocalized protein phonons. There is an assumption that the shape of the latter spectrum is the same for all chemically equivalent molecules in a bulk sample. So in this situation it can be referred to as the homogeneously broadened single site absorption spectrum. The analytical expression for the low – temperature single site absorption and fluorescence spectra of a chromophore embedded into an amorphous protein matrix using the equation is presented below [36].

L(( ) + — (2)

In Eq. 2, the - and + signs correspond to absorption and fluorescence. The first term shows the ZPL with Lorentzian shape at a frequency position The phonon wing consists of all one – phonon and multi – phonon transitions forming the – terms with (R 1) [36].

4.5. Inhomogeneous broadening

As already given in introduction part, a direct experimental determination of single site spectra of photosynthetic pigment – protein complexes (check Fig. 8, red line in Frame A) can only be gotten by low – temperature single molecule spectroscopy. This determination is still a challenging task, but a number of successful single molecule spectroscopy have been reported since 1999 [37, 38, 39, 40]. The conventional absorption and fluorescence spectra are widely structure

less because of serious inhomogeneous broadening of optical transitions of the pigments embedded in amorphous protein matrices and this feature should not be missed [8, 36].

Roughly, broadening mechanisms are considered to be *homogeneous* when affecting an optical transition of all molecules in an ensemble in the same way. Consequently, single – molecule spectra are by definition homogeneously broadened spectra. Ensemble spectra occur to be inhomogeneously broadened due to the specific environment of a pigment embedded into an amorphous matrix may differ from protein to protein in a bulk sample. In this case the transition frequency of that molecule is affected. Static inhomogeneous broadening of photosynthetic pigment – protein complexes is often well approximated by a nearly Gaussian distribution with full width in the order of 80 - 200 [8] that is referred to as inhomogeneous distribution function (IDF) [36].

The common similarities between the homogeneously and inhomogeneously broadened spectra are presented by model simulations in Fig. 8, Panel A. The bold red line shows the homogeneously broadened spectrum which is calculated according to Eq. 2. Dashed – dotted line represents the intensities of the ZPL which are distributed according to a Gaussian IDF with Bold blue line shows the inhomogeneously broadened absorption spectrum. As was noticed before, the experiments performed under non – line - narrowing conditions, the latter spectrum seems to be widely structure less The spectral resolution of conventional spectroscopy is in the order of so that the separation of ZPL and PSB feature ( ) is completely masked by relatively broad IDF. The only plain signature of the electron – phonon coupling is a slight asymmetry of the inhomogeneously broadened spectrum towards higher energies. Moreover, there is shift between the purely electronic transition at the center of the IDF and the absorption maximum, indicated as . Since absorption and fluorescence spectra are expected to be mirror symmetric the ZPL, the shift between absorption and fluorescence maxima, referred to as *Stokes shift.* So this shift can in the mean phonon frequency approximation estimated to be equal to twice the reorganization energy [36].

(3)

The width of the non – line- narrowed absorption spectrum is approximately [39].

+ (4)

It is obvious from the simulations presented in Fig.8 that any phonon structure is hidden by inhomogeneous broadening in conventional spectra. In this case spectrally selective experimental techniques are necessary to unravel information on electron - phonon coupling in photosynthetic pigment – protein complexes. It is believed that the static fluctuations of environment are the main cause of inhomogeneous broadening of optical spectra. They can formally be looked at as a kind of random noise that modulates the molecular transition energies [36].

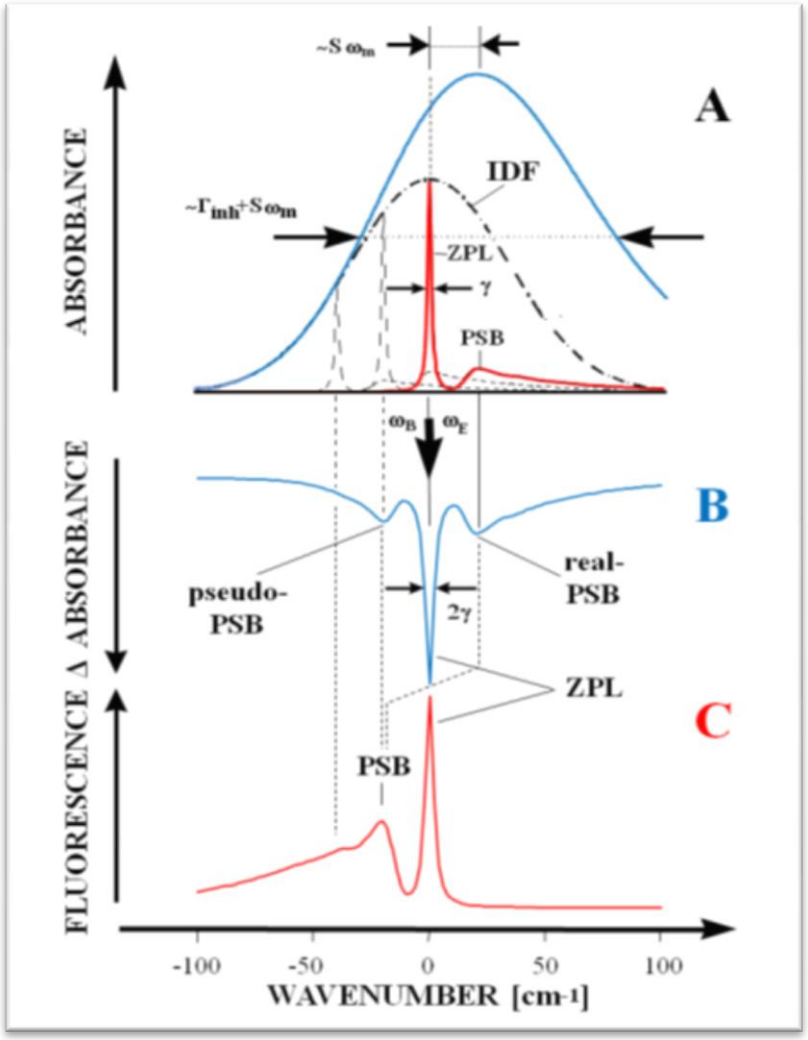

Figure 8. Illustration of conventional (Frame A) and line-narrowing spectroscopies (Frames B and C). **Frame A**: The red line represents the homogeneously broadened absorption spectrum of a model pigment-protein complex which include ZPL and an asymmetric PSB towards higher energies at low temperature. The convolution of the homogeneously broadened absorption spectrum with a Gaussian IDF shown as a dashed dotted line.
Frame B represents a SHB spectrum of the model pigment-protein complex which was shown in Frame A (blue line). It has ZPL and real-PSB towards the high-energy side of the ZPL.
Frame C shows a FLN spectrum of the model pigment-protein complex introduced in Frame A (red line). It consists ZPL and only a single PSB towards the low-energy side of the ZPL. This structure is because both, real-and pseudo-PSB, are found at the same side of the ZPL in the case of FLN.(According to [36]).

In a frame B the latter features correspond to the homogeneously broadened absorption spectrum and appear because of resonant burning of pigment molecules, whose ZPL are resonant with the burn frequency ω_B (presented as the red spectrum in Frame A). Also, the additional pseudo-PSB lying towards the low-energy side of the ZPL is the result of non-resonant burning of pigment molecules. PSB of these molecules are resonant with the burn frequency ω_B (presented by the dashed spectra in Frame A). Similarities between features given in Frames A and B are shown by full and dashed lines for the cases of resonant and non-resonant burning. [36].

4.6. Phonon structure in selectively excited spectra

All line- narrowing techniques such as SHB, FLN, delta – FLN are based on selective laser excitation within an inhomogeneously broadened absorption profile at low temperatures. This excitation selects the information from only a subset of pigment molecules absorbing at a certain burn/excitation frequency. The transition frequency of those molecules in SHB experiments selected by the burn laser is altered. That's why the difference between pre- and post- burn absorption spectra reveals a hole at the burn frequency and a concomitant increase of absorption at another frequency [36].

In a Fig.8 is shown a SHB spectrum for a model pigment – protein complex. This spectrum shows a sharp zero – phonon hole (ZPH) at the burn frequency ω_B and different PSB holes on the low- and high-energy sides of the ZPH. In Fig.8 *a* Frame A shows a comparison of the single site absorption spectrum with PSB where the ZPL is due to resonantly burned electronic transitions overlapping the burn frequency ω_B. The feature at the high – energy side of the ZPH is the real – PSB, that is because of the phonon wings of the resonantly burned ZPH. Consequently, ZPH and real – PSB correspond directly to ZPL and PSB of the homogeneously broadened absorption spectrum and presented on Fig. 8 Frame A as a bold red line. Moreover, there are electronic transitions within the IDF, that are non-resonantly overlapping the burn frequency ω_B via their phonon wings (check dashed lines in Frame A of Fig.8). Frame C of Fig.8 shows the corresponding FLN spectrum. The latter spectrum demonstrates a ZPL and only a single PSB feature [36].

After all above consideration it can be made a conclusion that real - and pseudo – PSB are mirror symmetric, that is valid only in cases where the inhomogeneous width is much larger than the width of the one-phonon profile

A delta – FLN spectrum is calculated as the difference between FLN spectra recorded before and after an intermediate hole burning step. There are two advantages in this technique in comparison with the traditional SHB and FLN spectroscopy: first, the scattered laser light that otherwise obscures the ZPL in FLN spectra can be effectively eliminated in the difference

spectrum, giving the opportunity of the direct measurement of the ZPL; second, the "double section" via both SHB and FLN suppresses the pseudo – PSB term in the low – fluence limit, and the final delta – FLN becomes identical to the homogeneously broadened spectrum [36].

Theoretically, the delta – FLN spectrum is obtained by substracting pre- and post – burn FLN spectra according to delta – FLN (ω) = FLN (, ω) – FLN (, ω). The post burn spectrum can be written as

( ) ( ) d (5)

Since that Eq. 5 contains two absorption line shapes: first, L due to the hole burning process, and second, due to the selective excitation of the post burn FLN spectrum. This difference leads to the "double selection effect" in delta- FLN. It has been shown theoretically that Eq. 5 reduces to Eq. 2 in the low fluence limit, i.e. the low-fluence delta-FLN spectrum is almost identical to the homogeneously broadened fluorescence spectrum. In this master thesis Eq. 2 is mostly used for calculations [36].

5. Experimental results

5.1. Comparison of Pre - burn FLN and Delta FLN

The spectra which were analyzed will be discussed now. Figure 9 shows pre-burn FLN and delta FLN spectra of PBP obtained with excitation wavelength of 635 nm within the PC absorption band.

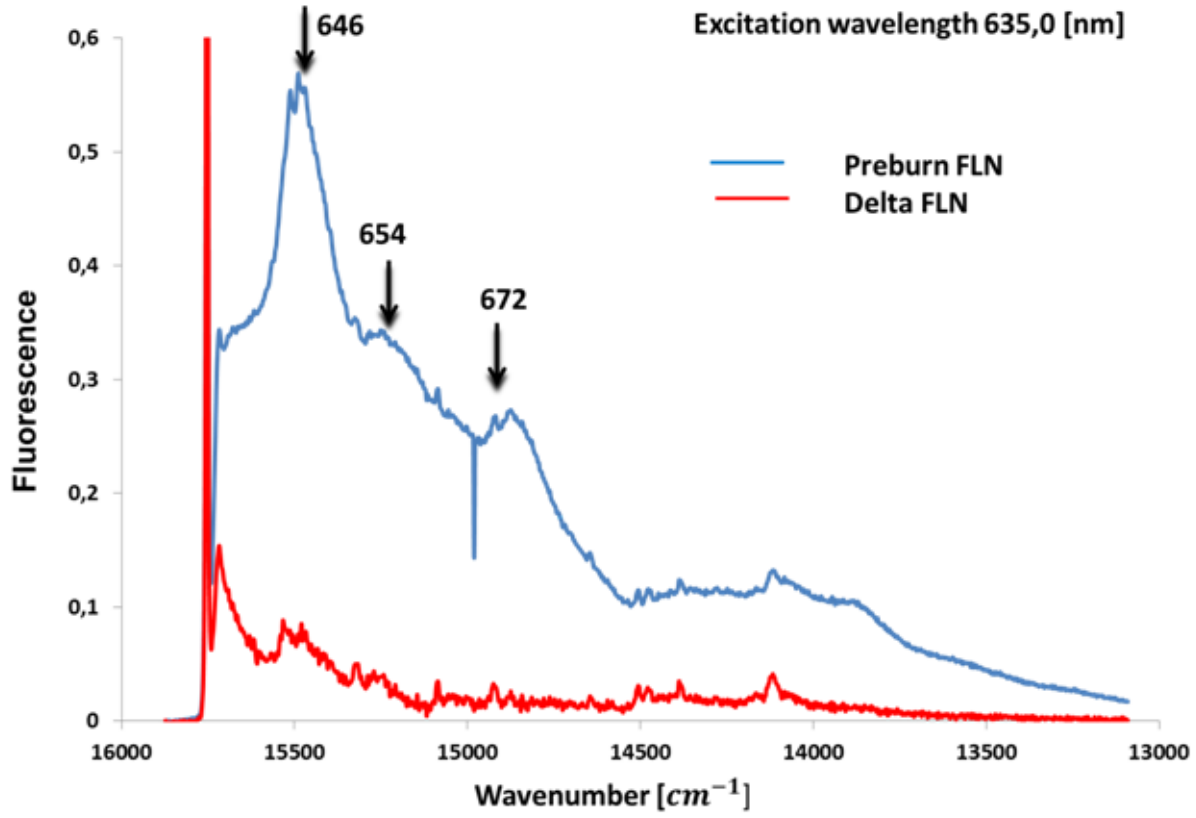

Figure 9. High – resolution pre-burn FLN (blue) and delta –FLN spectra (red) of phycobiliproteins obtained with an excitation wavelength of 635 nm at 4.5 K.

The pre - burn FLN spectrum contains three broad fluorescence bands at 646, 654 and 672 nm which still seem to be inhomogeneously broadened. Despite of the narrow laser excitation this means they are due to energy transfer. In addition to these broad features there are some narrow features, corresponding to vibrational lines. But for instance here there is no resolved phonon side band. This means the pre- burn FLN has no full selectivity reached.

Delta FLN has no broad features any more, but it has a distinct PSB (phonon side band) and the peak is at 34 cm^{-1}. There are a lot of distinct narrow vibrational lines which are resolved. So it means that delta FLN spectra reached full selectivity and it corresponds to the homogeneously

broadened fluorescence spectrum at the wavelength of 635 nm. The wavelength of 635 nm corresponds to PC.

Figure 10. represents pre-burn FLN and delta FLN spectra of PBP obtained with excitation wavelength of 645 nm.

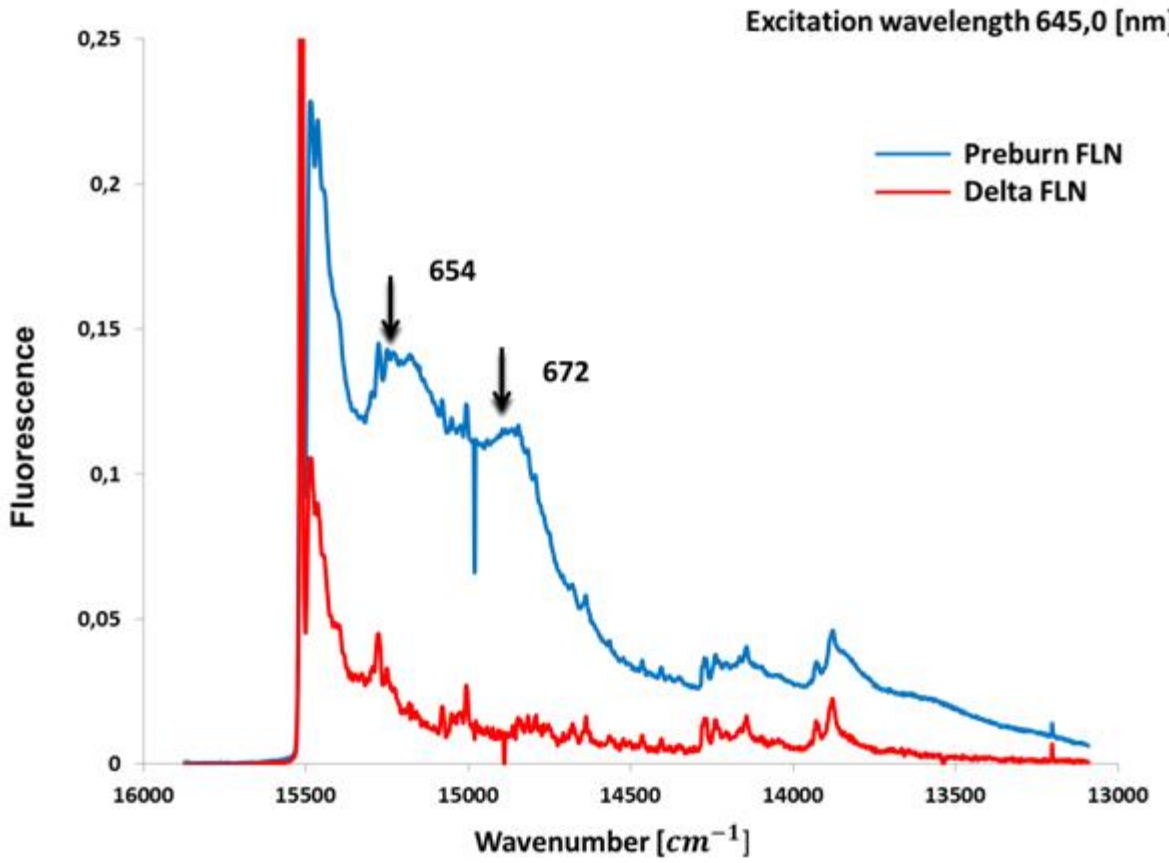

Figure 10. High – resolution pre-burn FLN (blue) and delta –FLN spectra (red) of phycobiliproteins obtained with an excitation wavelength of 645 nm at 4.5 K.

Pre - burn FLN spectrum has two broad fluorescence bands at 654 and 672 nm which still seem to be inhomogeneously broadened. This means there is still EET from the excitation wavelength to electronic states associated with the latter inhomogeneously broadened bands. Also there are some narrow features, corresponding to vibrational lines. PSB is clearly visible. Since there are still broad features full selectivity is not reached.

There are no broad features in delta FLN spectra, but it has a distinct PSB and the peak is at 31 cm^{-1}. Also as previous delta FLN at 635 nm it has large number of visible vibrational lines. Delta FLN spectra reached full selectivity and it corresponds to the homogeneously broadened fluorescence spectrum at the wavelength of 645 nm which corresponds to APC.

Figure 11 represents pre-burn FLN and delta FLN spectra of PBP obtained with excitation wavelength of 650nm.

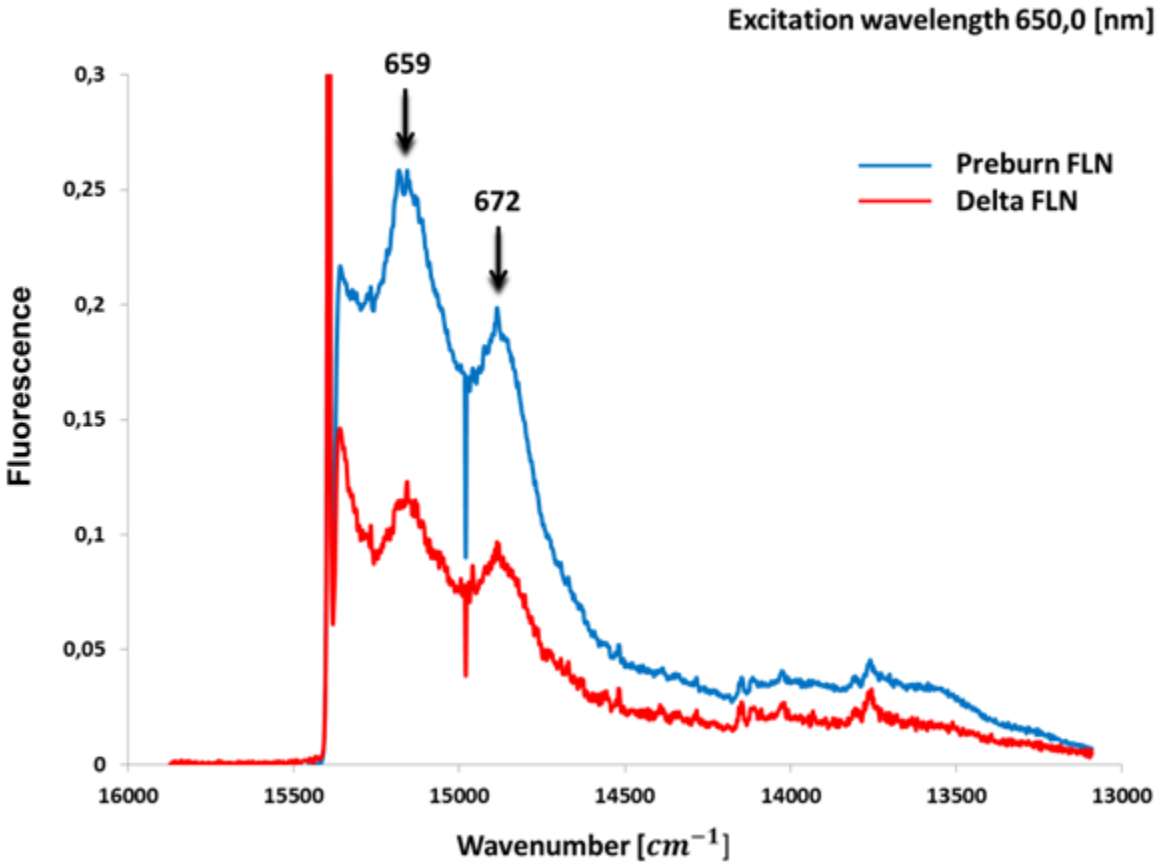

Figure 11. High – resolution pre-burn FLN (blue) and delta –FLN spectra (red) of phycobiliproteins obtained with an excitation wavelength of 650 nm at 4.5 K.

Pre - burn FLN spectra has two broad fluorescence bands at 659 and 672 nm which still seem to be inhomogeneously broadened despite of the narrow laser excitation. This means there is still EET from the excitation wavelength to electronic states associated with the latter inhomogeneously broadened bands. Narrow features are clearly visible and correspond to vibrational lines. PSB is hardly resolved because its overlaps with closely spaced electronic state.

Delta – FLN at 650 nm has more resolution because the phonon side band is clearly visible. Also delta – FLN has two broad features from EET this means that energy state from one to another is very efficient.

Figure 12 shows pre-burn FLN and delta FLN spectra of PBP obtained with excitation wavelength of 675 nm.

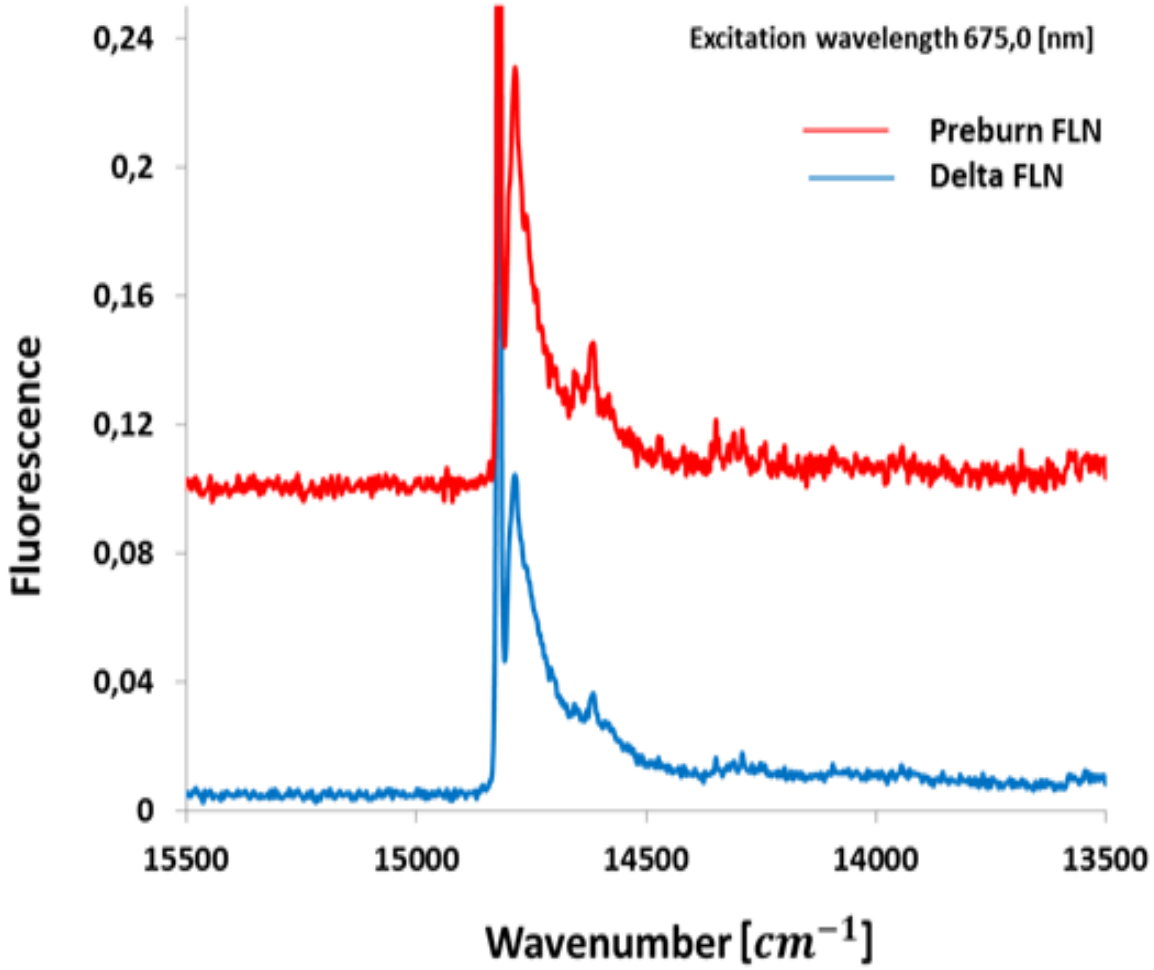

Figure 12. High – resolution pre-burn FLN (blue) and delta –FLN spectra (red) of phycobiliproteins obtained with an excitation wavelength of 675 nm at 4.5 K.

Figure 12 shows no inhomogeneously broadened bands the excitation wavelength of 675 nm. So it visible only phonon and vibrational structure is visible, which include phonon side band and narrow line. That shows no more energy transfer.

5.2. Electron ïvibrational frequencies of PBP of *A.marina*

Fig.14 represents the plot of different delta-FLN spectra excited at wavelength from 635 nm to 675 nm. The most intense vibronic lines are labeled by their frequencies in units of wavenumbers. All discernible vibronic lines correspond most probably to localized vibrations of the the phycocyanobilin (PCB) pigment molecules bound by phycobilibroteins in *A. marina.*

The characteristic vibrational frequencies for phycobiliproteins of *A. marina* are summarized in Table 5.1. Fig. 13 shows the molecular structure of PCB .where the bond between the C_{19} and C_{20} molecules is highlighted by a blue circle.

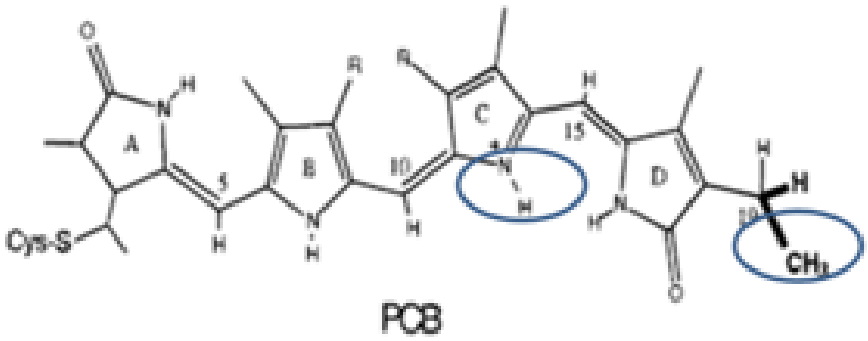

Figure 13. Molecular structure of phycocyanobilin (PCB)

The bond between the C_{19} and C_{20} molecules is highlighted by a blue circle in a Figure 13.

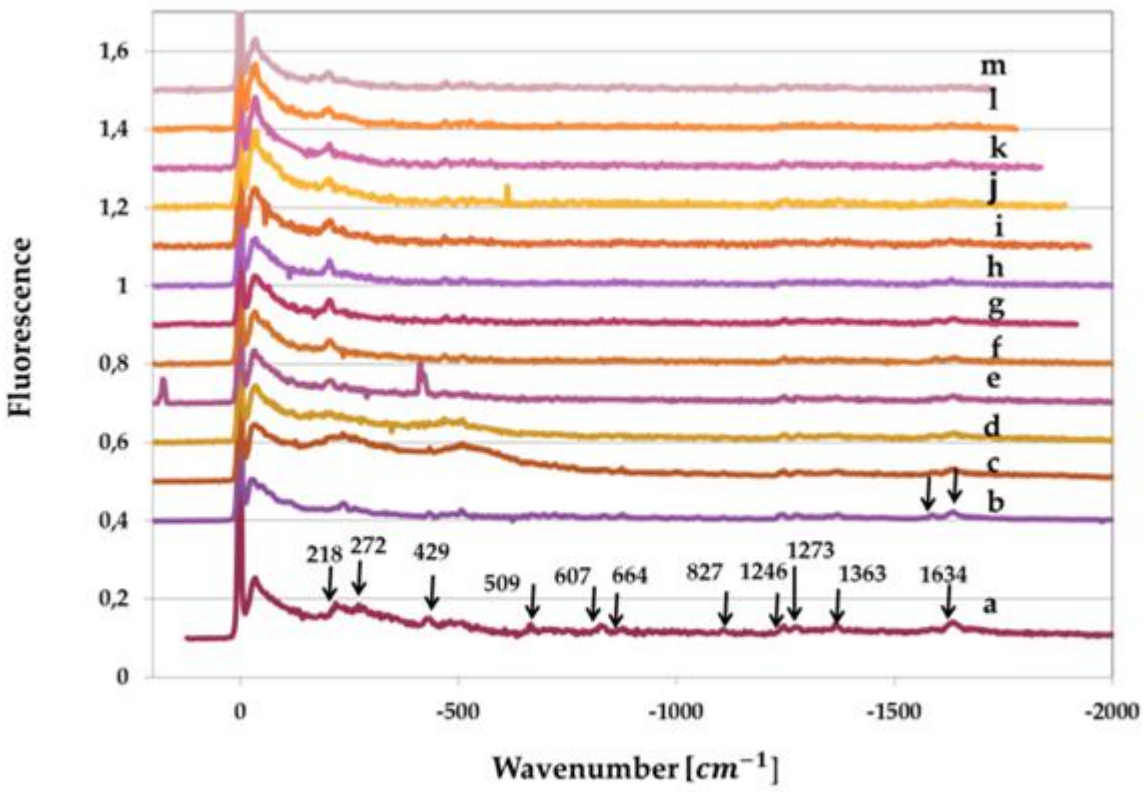

Figure 14. Plot of difference fluorescence spectra obtained for wavelength from 635 to 675 [nm]. The labels a-m correspond to the excitation wavelength, i.e. 635 (a), 645 (b) 650 (c), 652,8 (d), 655,3 (e), 657,5 (f), 660,2 (g), 662,8 (h), 665,2 (i),667,7 (j), 670,2 (k), 672,8 (l) and 675 nm (m). Arrows give vibrational frequencies in wavenumbers.

Overall, the vibrational frequencies obtained at different excitation wavelengths are rather similar. This finding indicates that the same type of pigment molecule is responsible for the five fluorescent electronic states assigned above. The obtained frequencies were compared with the resonance Raman spectra of PCB in recombinant phytochrome (Table 5.1), i.e. the same chromophore but embedded into a different protein matrix [36]. In the range of H-out-of-plane-wagging modes (~800 cm^{-1}) and N-H- and C-H-rocking modes (~1300 cm^{-1}), there is only a qualitative agreement of the observed vibrational frequencies, which is most probably due to the different protein environment in PBP complexes.

Two important modes at 1634 and 1580 cm^{-1}, respectively, listed in Table 5.1 agree very well with those observed for PBP complexes and are a very characteristic for phycocyanobilin. The mode at 1634 cm^{-1} is associated with a stretch motion between two carbon atoms. Another mode is 1580 wavenumber and it corresponds to C-NH^{+} stretch motion. This motion is absent at 635 nm, this can be explained by a specific environment that suppresses this mode so that maybe the environment is different which is consistent with assigning this pigment to PC, while the chromophore at 645 nm can be assigned to APC.

.

Table 5.1. Vibrational frequencies of different wavelength in comparison with Raman spectroscopy paper

PCB in phytochrome **(Andel et. al. Biochemistry 2000, 2667 - 2676)**		**635 nm**	**645 nm**	**650 nm**	**652,8 nm**	**655,3 nm**	**657,5 nm**	**660,2 nm**	**662,8 nm**	**665,2 nm**	**667,7 nm**	**670,2 nm**	**672,8 nm**	**675 nm**	**677,7 nm**	**680 nm**
	PSB	34	31	34	36	32	32	33	36	34	37	34	37	35	31	38
						210	204									
		218	234	237	231	240	234	241		235						
		272		267	282											
								348								
						413		400								
		429	432	434	432	422		429								
					468		469	474	471	468		470	470		457	456
493		482														
		509	506	507	508	509	511	513	507	529	509	511	508			
		543	536													
		607		612		608										
665		664	665	668	665											
			697	700	696	706	702			708						
762	**C-H out of plane wagging modes**		723	722	716	725	727	735		730	720	730	729		744	759
801		827	834	838	841	830	826	827			826	856	842		848	848
873		877	877	876	876	877	874	856	858	855	878	874	874			
										873	891		902			
											966	966			951	950
					1007	1011		1023		1034	1024	1011	1000			1020
					1052	1053	1057	1059	1064	1077	1075	1075	1060		1088	1088
						1163					1148	1149	1144			1187
1224	**C-H / N-H rocking modes**	1246	1240	1245	1249	1249	1249	1243	1249	1248	1254	1242	1241	1241	1261	
1295		1273	1272	1273	1282	1274	1287	1289	1286	1290	1290	1288	1289	1280		
1318																
1379		1363	1370	1366	1369	1368	1374	1373	1370	1365	1373	1374	1374	1386	1391	1391
												1500				
1571	**C=N stretching**		1583	1589	1589	1588	1595	1596	1594	1590	1591	1601				
1634	**stretching**	1634	1634	1638	1638	1634	1638	1639	1631	1629	1629	1631	1633	1628	1634	1633

5.3. Electron ïphonon coupling

The dynamics of energy transfer and relaxation processes is mostly determined by the quasi – continuum phonon part of the spectral density. That's why the total coupling strength of phonons to an electric transition, controlling the intensity distribution between the ZPL and the PSB, has a special interest It is characterized by a single dimensionless number, the Huang – Rhys factor S. The Huang - Rhys factor is associated with the displacement of the equilibrium positions of the nuclei upon a photo excitation of the chromophore. Consequently, S is a measure for the strength of the linear electron – phonon coupling and characterizes the average number of phonons accompanying a particular electronic transition.

Electron – phonon coupling studies were carried out by using like fluorescence line narrowing spectroscopy at low temperature. In this part will be given a detailed characterization of electron-phonon coupling of phycobiliproteins of *A. marina* using delta-FLN experiments. Shortly, a delta-FLN spectrum is determined as the difference between two FLN spectra recorded before and after spectral hole burning. In comparison to "conventional" FLN, this subtraction technique gives ZPL virtually free from scattering artifacts of the excitation laser beam so that electron-phonon coupling strengths can be directly determined.

Figure 15 (left side) shows the fits according to equation 5 of delta-FLN spectra obtained at different burn fluences the excitation wavelength of 635nm.

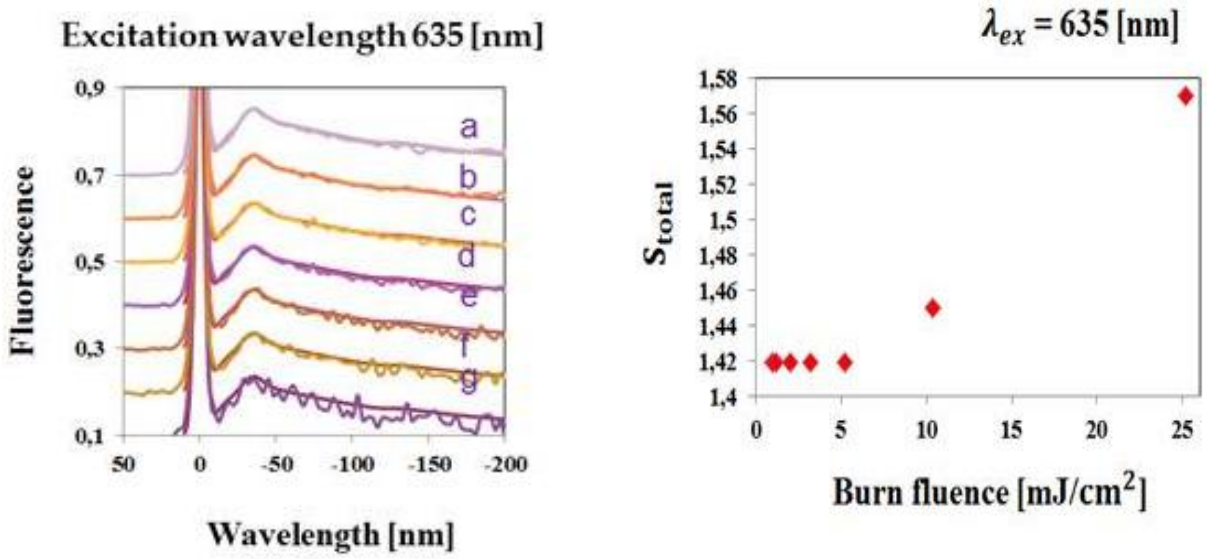

Fig. 15 Fit of delta-FLN spectra obtained at different burn fluences (a – 1; b – 1,2; c – 2; d – 3,2; e – 5,2; f – 10,4 and g – 25,2 mJ/cm^2) (left side) and plot of corresponding S factors (right side) at the excitation wavelength of 635 nm.

The main difference between all spectra is different burn fluence. The highest fluence has the best signal to noise ratio so the lineshape was estimated and kept constant. After that all fluences were fitted and S factor was obtained. The line shape describes the properties of environment of a chromophore which was tested. The different S factors obtained were plotted as a function of fluence (see Figure 15 righ side). From the S factor plot it is obvious that the S-values decrease with decreasing fluence. This indicates that the S factor was overestimated at high burn fluence and the S-factor comes to a constant limit at low fluence. From this observation it can be made a conclusion that real S factors are observed in the low frequency limit.

Delta – FLN spectra were selectively excited at several wavelengths within the fluorescence – origin bands ranging from ~ 635 up to 675 nm. The phonon (PSB) region of several of these delta –FLN spectra are shown as brown curves in Figure 16, where the dark blue curves correspond to theoretical fits according to equation 2. All spectra were analyzed as discussed before for the excitation wavelength of 635nm, however, only the highest fluence spectra and respective fits are shown in Figure 15 for brevity, which show a rather good agreement of the fit with the data. Proper fits required the assumption of three individual one-phonon profiles, each characterized by a separate mean phonon frequency and one-phonon profile composed of a Gaussian at its low-energy wing and a Lorentzian at the high-energy wing. Table 5.2 represents the Huang – Rhys factors S and corresponding parameters of the one-phonon profiles of phycobiliproteins of A. marina obtained by the fits of delta –FLN spectroscopy at 4.5 K. Figure 17 represents S total dependence at excitation wavelength from 635 to 675 nm. The latter plot and Table 5.2 show that all identified electronic states at 635 (PC), 645 (APC), 654, 659, and 672 nm, respectively, are characterized by different S-factors and partly by different mean phonon frequencies and/or one phonon profiles. Since the one-phonon profile characterizes the environment of a given chromophore, the latter finding suggests that the pigment molecules responsible for the above low-energy states are embedded into different protein environments. Within each electronic state, the S-factor seems to decrease with increasing excitation wavelength, which could be due to residual EET from overlapping higher energy states at the blue side of the individual absorption band of a given electronic state.

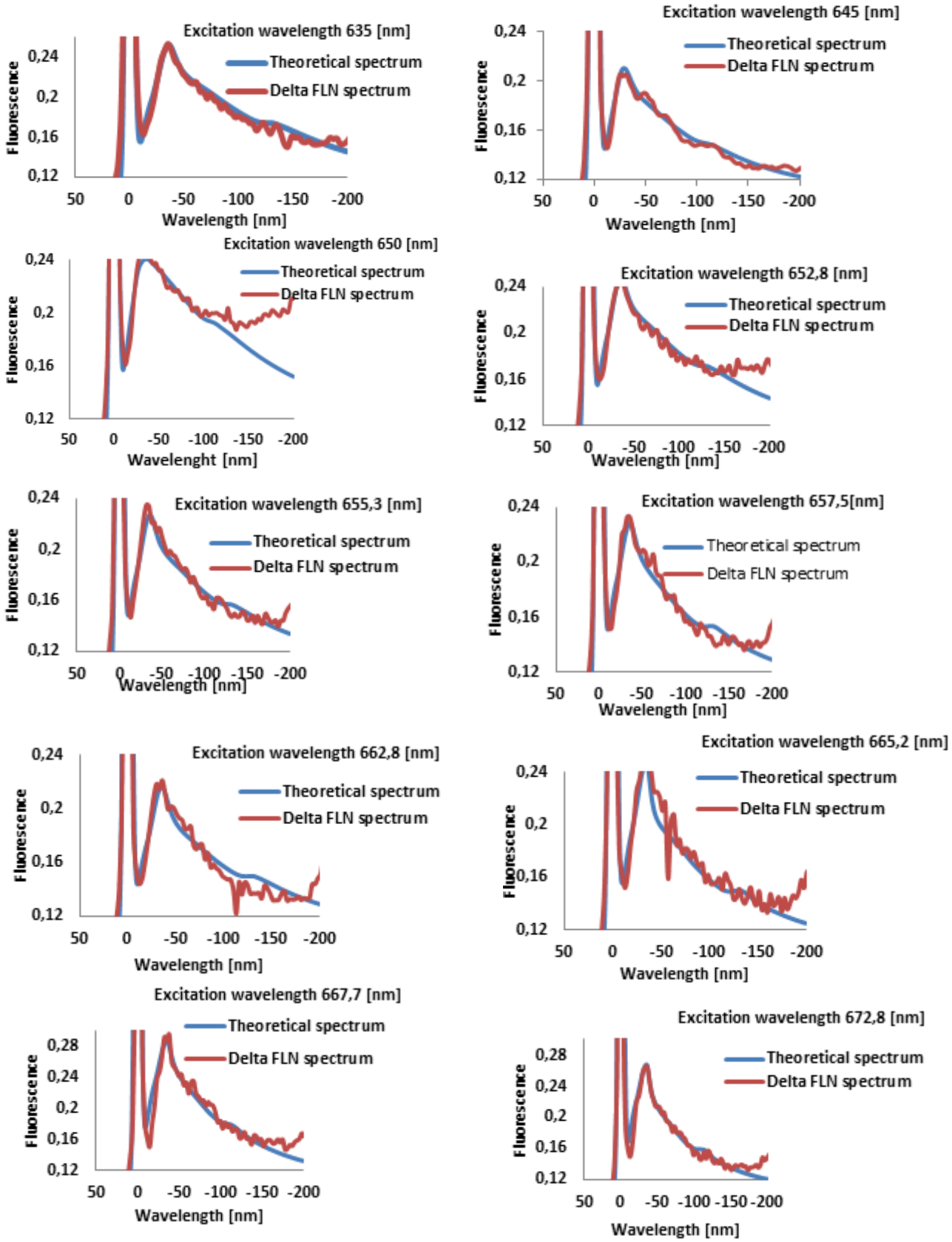

Figure 16.Typical 4.5 K delta- FLN spectra (brown curves) of phycobiliproteins of A. marina excited/burned in the wavelength range between 635 and 672,8 nm and recorded with a fluence of ~2 mJ/cm ^{2}. The fluence applied for hole-burning was 25 mJ/cm ^{2}. The actual excitation/burn wavelength is given in each frame. The blue curves show fits (according to equation 2).

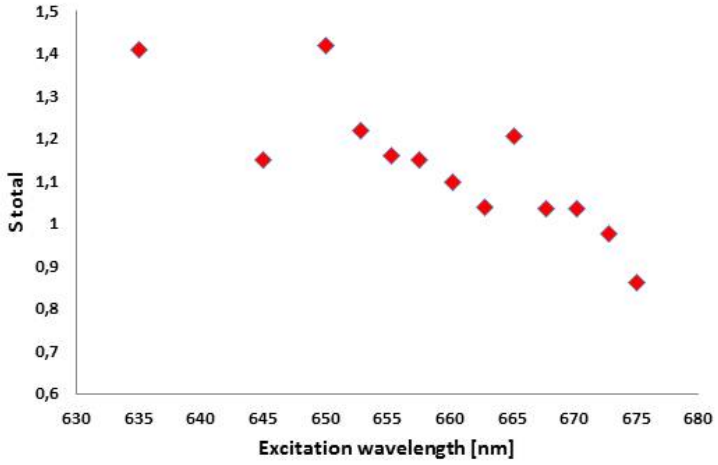

Figure 17. S total dependence at excitation wavelength from 635 to 675 nm

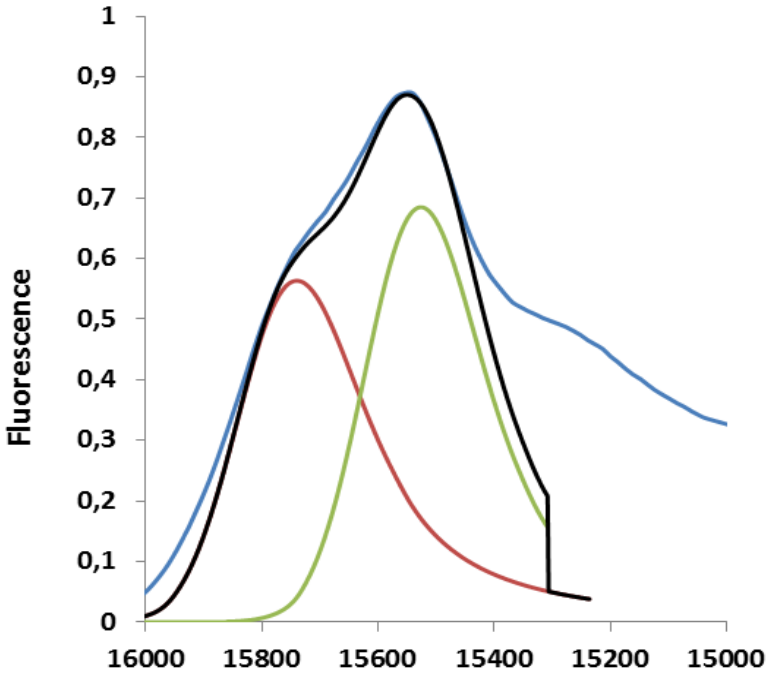

Figure 18. Fit of fluorescence assuming two fluorescence bands for PC and APC, respectively, characterized by the electron-phonon coupling parameters given in Table 5.2

Figure 18 shows the spectrum that was calculated for comparison of parameters for electron – coupling for PC and APC and checking if they are correct. The fluorescence bands were calculated and fitted to the measured fluorescence spectrum (blue line). Brown line represents calculated PC fluorescence spectra, when the green line is calculated APC fluorescence spectra. Black spectra represent a sum of PC and APC fluorescence spectrum. The overall agreement is quite good, which is a proof for the quality of the reported electron-phonon coupling parameters.

Table 5.2. Huang – Rhys factors of phycobiliproteins of *A. marina* obtained by delta – FLN spectroscopy at 4.5 K

Ex.Wavelenght[nm]	635	645	650	652,8	655,3	657,5	660,2	662,8	665,2	667,7	670,2	672,8	675
S total	1,42	1,15	1,42	1,22	1,16	1,15	1,09	1,04	1,21	1,035	1,035	0,98	0,86
S unc	0,1	0,12	0,14	0,12	0,12	0,12	0,12	0,14	0,16	0,14	0,14	0,16	0,16
Profile 1													
Huang-rhys factor	1,22	1	1	1,05	1	1	0,96	0,9	0,9	1,05	0,9	0,85	0,75
Peak phonon frequency [	20	20	25	20	20	20	20	20	20	20	20	20	20
FWHM of Gaussian wing	25	25	25	25	25	25	25	25	25	25	25	25	25
FWHM of Lorentzian wing]	160	140	120	160	160	140	140	160	120	100	90	90	160
Profile 2													
Huang-rhys factor	0,043	0,03	0,037	0,031	0,036	0,03	0,0143	0,03	0,026	0,031	0,025	0,025	0,022
Peak phonon frequency [	134	115	115	134	134	134	134	115	115	115	115	115	115
FWHM of Gaussian wing	20	20	20	20	20	20	20	20	20	20	20	20	20
FWHM of Lorentzian wing]	60	60	60	60	60	40	40	60	30	30	20	20	20
Profile 3													
Huang-rhys factor	0,156	0,12	0,126	0,139	0,125	0,12	0,124	0,11	0,122	0,125	0,11	0,102	0,09
Peak phonon frequency [	35	28	30	35	35	35	35	35	35	35	37	37	37
FWHM of Gaussian wing	20	15	15	20	20	20	20	20	20	20	20	20	20
FWHM of Lorentzian wing]	20	20	15	20	20	20	20	20	10	15	10	10	10

6. Discussion

Delta – FLN spectroscopy at 4.5 K has been used to investigate electron – phonon and electron – vibrational coupling strengths of the lower excitation level of the phycobiliproteins of A. marina. The results presented characterize electron - phonon and electron – vibrational coupling of PBP.

Pre-burn FLN spectrum show the existence of inhomogeneously broadened bands which can be assigned as electronic states populated by energy transfer. Based on these data, five different electronic states can be identified at 635 (PC), 645 (APC), 654, 659, and 672nm, respectively. The states at 654 and 659 nm are previously unresolved electronic states in the spectral region between APC and the terminal emitter (Theiss et al. 2011). At first glance, the observation of five different fluorescent statesin an antenna complex seems to be surprising, because it indicates that in some of the PBPs in the bulk solution EET is interrupted at low temperature in the presence of glycerol (Theiss et al. 2011).

The observed vibrational frequencies do not change much with excitation wavelength between 635 and 675 nm indicating that the chromophores responsible for all observed electronic states are most probably the same. However, two intense modes are observed at 1634 and 1580 cm^{-1}, respectively, which are characteristic for the phycocyanobilin pigment (Andel et.al.). The mode at 1580 cm^{-1} corresponds to a C- NH^{+} stretch motion. This mode is absent at 635 nm, which can be explained by a specific environment in PC that may suppress this mode. The vibronic band at 1634 cm^{-1} represents the $C_{19} – C_{20}$ stretching mode (Andel et.al.). PBP also shows vibronic bands at 1246, 1273 and 1363 cm^{-1}, respectively, in the region of N – H and C- H rocking modes. In the region of H – out of plane wagging modes, PBPs exhibit vibronic bands at 723 and 834 cm^{-1}. These vibrational frequencies differ from those reported from Raman experiments on PCB embedded in phytochrome (Andel et.al.) indicating that the specific environment of the PBP antenna influences the positions of the of N – H and C- H rocking modes as well as the H – out of plane wagging modes.

As for electron – phonon coupling, delta – FLN spectra were measured at several wavelengths within the fluorescence – origin bands ranging from ~ 635 up to 675 nm. All identified electronic states at 635 (PC), 645 (APC), 654, 659, and 672 nm, respectively, are characterized by different S-factors and –in part- by different mean phonon frequencies and/or one phonon profiles. Within the inhomogeneously broadened band of each electronic state, the S-factor seems to becaome smaller with increasing wavelength, which may be due to EET from overlapping higher energy states at the blue side of the absorption band of any of the identified electronic state leading to an artificial increase of S.

The lineshapes of the one-phonon profile are characteristic for protein environment of a certain chromophore. Therefore, the finding of different one-phonon profiles for each of the above identified electronic states indicates that the pigment molecules responsible for the respective low-energy states are bound in different protein environments. So it can be concluded that the additional electronic states observed at 654, 659, and 672 nm are not located in PC and/or APC and are lying. lower in energy than states corresponding to APC (Theiss et al. 2011). One possible conclusion is to assign the electronic states at 654, 659, and 672 nm to pigment molecules bound by the linker.

7. Summary

Main goal of this thesis was to get better understanding of EET in PBP of *A.marina*. The results of time-resolved spectroscopy have to be supplemented by investigations of spectral positions and excitonic nature of excited electronic states and of electron-vibrational coupling.

Parameters of homogeneously broadened spectra using site-selective spectroscopies like difference fluorescence line - narrowing (ΔFLN) and spectral hole - burning (SHB) were obtained. The present study is based on application of SHB and ΔFLN spectroscopy for an investigation of excited state positions as well as homogeneous and inhomogeneous broadening of PBP.

Excitation energy transfer and electron-vibrational coupling in PBPs have been investigated by selectively excited fluorescence spectra. The data reveal a rich spectral substructure with a total of five low-energy electronic states including a terminal emitter at about 672 nm. Furthermore, a large number of vibrational features can be identified for each electronic state with intense phonon sidebands peaking at about 30 cm^{-1} and e.g. two characteristic vibronic lines at about 1580 and 1634 cm^{-1}, which appear to correspond to C-NH+ and C-C stretching modes of the bilin chromophore, respectively. The exact phonon and vibrational frequencies vary with electronic state implying that the respective chromophores are bound to different protein environments. A possible structural assignment of the electronic states will be discussed.

In future is planned to continue research of EET in the PBP antenna of *A. marina.*

The results obtained provide valuable information for a further understanding of EET in the PBP antenna of *A. marina*.

8. Summary in Estonian

Käesoleva töö põhieesmärgiks oli paremini mõista ergastusenergia ülekannet *Acaryochloris marina* fükobiliproteiinides. Selleks uuriti ergastatud elektronide joonte asukohti aeglahutatud spektroskoopias, ergastuse iseloomu ja elektron-vibratsioonilist vastastikmõju.

Kasutades selektiivseid spektroskoopiaid nagu selektiivne fluorostsentsspektroskoopia (ΔFLN) ja spektraalsälkamine (SHB), saadi homogeenselt laienenud spektrite parameetrid. Käesolev töö põhineb eelmainitud spektroskoopiate rakendamisel, uurimaks nii ergastatud olekute asukohti kui ka homogeenset ja ebahomogeenset fükobiliproteiinide joonte laienemist.

Ergastusenegria ülekannet ja elektron-vibratsioonilist vastastikmõju fükobiliproteiinides uuriti selektiivselt ergastatud fluorestsentsspektritega. Andmed näitavad rikkalikku spektraalset alamstruktuuri viie madalaenergilise eletroonse olekuga, sealhulgas kiirgust 672 nm juures. Lisaks saab iga elektroonse oleku jaoks identifitseerida suure hulga vibratsioonilisi karakteristikuid intensiivse foononi kõrvalpiikidega umbes 30 cm^{-1} juures ja näiteks kaks iseloomulikku vibratsioonilist joont 1580 ja 1634 cm^{-1} juures. Need jooned vastavad C-NH+ ja C-C sidemete valentsvõnkumistele fükobiliini kromofooris. Täpsed foononi ja vibratsioonilised sagedused varieeruvad koos elektroonse olekuga, viidates sellele, et vastavad kromofoorid on seotud erinevate valguliste keskkondadega. Võimalike elektroonsete olekute struktuurne määramine on arutamisel.

Tulevikus on plaanis jätkata ergastusenergiate ülekande uurimist *A. marina* fükobilivalgulises antennikompleksis.

Saadud tulemused annavad väärtuslikku informatsiooni, et täpsemalt mõista ergastusenergia ülekannet *A. marina* fükobilivalgulises antennikompleksis.

9. Acknowledgment

Hereby, I would like to acknowledge the following people and organization that has contributed immensely in making this master thesis realizable and my stay and study in Estonia worth the while.

Firstly, is my supervisor of master thesis professor Jörg Pieper whose guidance was of great benefits to me. He provided assistance throughout the research work and was always available and had listening ears on how to find solutions to any problem that arises during the cause of writing the thesis.

Moreover, worthy of mention is Dr. Margus Rätsep (UT Tartu) who in the experimental section carried out experiments that for the analysis. Samples were provided by Dr. Hann-Jörg Eckert, Sabine Kussin and Monika Wess (all TU Berlin) to them all I say great thank you.

This acknowledgement will not be complete if I fail to mention the financial support provided by the Estonian Research Council (Grant ETF 9453) your financial support is appreciated.

Above all, I thank God for his mercies and grace in seeing me through all this period of study in Estonia .

10. References

1. Grossman, A. R.; Bhaya, D.; Apt, K. E.; Kehoe, D. M. *Ann. Rev. Genetics* 1995, 29, 231.

2. Miyashita, H.; Ikemoto, H.; Kurano, N.; Adachi, K.; Chihara, M.; Miyachi, S. *Nature* 1996, *383*, 402.

3. Larkum, A. W. D.; Kühl, M. *Trends in Plant Science* 2005, 10/8, 355 - 357.

4. Chen, M.; Quinnell, R. G.; Larkum, *A. W. D. FEBS Lett*. 2002, 514, 149.

5. Marquardt, J.; Senger, H.; Miyashita, H.; Miyachi, S.; Mörschel, *E. FEBS Lett*. 1997, p. 410, 428.

6. Purchase, R.; Völker, S. *Photosyn*. Res. 2009, 101, 245.

7. Aartsma, T.J., and J. Matysik, editors. *Biophysical Techniques in Photosynthesis. Springer*, Dordrecht, June 2008, Volume 46, Issue 2, 201.

8. Jankowiak, R.; Reppert, M.; Zazubovich, V.; Pieper, J.; Renoit, T. *Chem. Rev.* 2011, 8, 45-46.

9. Purves, W.K.; Orians, G.H.; Heller, H.C. *Life: The Science of Biology*, 4th Edition, by Sinauer Associates Inc., W. H. Freeman and Company,Sunderland, Mass.

`10. Wim, V. An Introduction to Photosynthesis and Its Applications. "The World & I" ,March 1998 issue, p. 158-165 (http://bioenergy.asu.edu/photosyn/education/photointro.html)

11. Seckbach, J. 2007.Algae and Cyanobacteria in Extreme Environments, 2007, 103,108.

12. Razeghifard, M. R.; Chen, M.; Hughes, J. L.; Freeman J.; Krausz E.; Wydrzynski, T. Spectroscopic studies of photosystem 2 in chlorophyll *d* – containing *Acaryochloris marina.* 2005, 1 – 2 (a-b).

13.Chen, M.; Quinnell, R.G; Larkum, A.W.D. The major light - harvesting pigment protein of *Acaryochloris marina.* . *FEBS Letters*, 2002, 149.

14 . Theiss, C.; Schmitt, F.J.; Pieper, J.; Nganou, C.; Grehn, M.; Vitali, M., Olliges, R.; Eichler, H. J.; Eckert, H.J. Excitation energy transfer in intact cells and in the phycobiliprotein antennae of the chlorophyll *d* containing cyanobacterium *Acaryochloris marina. Journal of plant physiology*, 168:(2011),1473 – 1487.

15. Akiyama, M., Miyashita, H., Kise, H., Watanabe, T., Miyachi,S. and Koboyashi, M. *Anal. Sci*. 2001,1 7 , p. 205 - 208.

16. Kobayashi, M.; Watanabe, S.; Gotoh T.; Koizumi, H.; Itoh, Y.; Akiyama, M. et al. Minor but key chlorophylls in Photosystem II. Photosynth Res 2005; 84 :201–7.

17. Hu, Q., Miyashita, H., Iwasaki, I., Kurano, N., Miyachi, S., Iwaki. M., et al. A photosystem I reaction center driven by chlorophyll d in oxygenic photosynthesis. Proc Natl Acad *Sci* 1998; 95:13319–23.

18. Kumazaki, S.; Abiko,K.; Ikegami, I.; Iwaki, M.; Itoh S. . Energy equilibration and primary charge separation in chlorophyll *d*- based photosystem I reaction center isolated from *Acaryochloris marina.* 2002, Elsevier Science B.V, 153 – 157.

19 . Gillbro, T.; Sandstrom, A.; Sundstrom, V,.; Wendler, J.; Holzwarth, A. R. Picosecond study of energy transfer kinetics in phycobilisomes of Synechococcus 6301 and the Mutant AN 112. *Biochim Biophys Acta*, 1985;808 :52–65.

20. Suter, G. W.; Holwarth A.R. A kinetic model for the energy transfer in phycobilisomes. *Biophys* J, 1987, 52: 1-12.

21. Marquardt, J.; Senger, H.; Miyashita, H.; Miyachi, S.; Mörschel, E. Isolation and characterization of biliprotein aggregates from Acaryochloris marina, a prochloron-like prokaryote containing mainly chlorophyll d. *FEBS Lett* 1997;410:428–32.

22. Suter, G.W.; Holzwarth, A.R. Structure–function relationships and energy transfer in phycobiliprotein antennae. Physiol Plant 1991; 83:518–28. A kinetic-model for the energy-transfer in phycobilisomes. *Biophys* , J 1987;52:673–83.

23. Chen, M.; Bibby, T.S.; Nield, J.; Larkum, A.W.D.; Barber, J. *FEBS Lett.* 2005, *579*, 1306.

24. Schmitt, F.; Theiss. C., Wache, K; Fuesers, J.; Andree S., Eichler, H. J.; Eckert H. J. Investigation of metabolic changes in living cells of the Chl d – containing cyanobacterium Acaryochloris marina by time – and wavelength correlated single – photon counting., 2007, 6-23.

25. Mullineaux, C.W. Phycobilisome - reaction center interaction in cyanobacteria. *Photosynth Res* ,2008 95:182-175.

26. Middepogu, A.; Murthy, S.D.S ; Reddy, P.B. Structural organization and functions of phycobiliproteins in cyanobacteria. International journal of plant, animal and environmental sciencesm, volume 2, issue- 2, april – june ,2012, 14 -9.

27. Wendler, J.; Holzworth, A. R.; Wehrmeyer, W . Picosecond time resolved energy transfer in phycobilisomes isolated from the red alga Porphyridium cruentum. *Biochim. Biophys*. Acta 1984, 765 :58-67.

28. Mimuro, M.; Akimoto, S.; Yamazaki, I.; Miyachi, H.; Miyashita, S. Fluorescence properties of chlorophyll d-dominating prokaryotic algae, Acaryochloris marina: studies using time-resolved fluorescence spectroscopy on intact cells. *Biochim Biophys Acta* 1999; 1412 :37–46.

29. Theiss, C.; Schmitt, F.J.; Andree, S.; Cardenas-Chavez, C.; Wache, K.; Fuesers, J. et al. Excitation energy transfer in the phycobiliprotein antenna of Acaryochloris marinastudied by transient fs absorption and fluorescence spectroscopy. *Photosynthesis:energy from the sun.* In: 14th International Congress on Photosynthesis.Dordrecht: Springer; 2008a, 339–42.

30.Pieper, J.; Rätsep, M.; Eichler, H. J.; Eckert, H. J. Low-energy level structure and electronphonon coupling of phycobiliproteins of the cyanobacterium Acaryochloris marina investigated by site-selective spectroscopy. *J Plant Physiol.*, 2011 Aug 15; 168(12):1473-87.

31. Hu, Q.; Marquardt, J.; Iwasaki, I.; Kurano, H.; Miyashita, N.; Mörschel, E. et al. Molecular structure localization and function of biliproteins in the chlorophyll a/d containing oxygenic photosynthetic procaryote Acaryochloris marina. *Biochim Biophys Acta* 1999; 1412 : 250–61.

32. Sauer, K.; Scheer, H. Exciton transfer in C-phycocyanin. Förster transfer rate and excitonic calculations based on new crystal structure data for C-phycocyanins from Agmenellum quadruplicatum and Mastigocladus laminosus. *Biochim Biophys Acta* 1988; 936 : 157–70.

33. Reppert, M.; Naibo, V.; Jankowiak, R. *J. Chem. Phys.* 2010, *133*, 1.

34 . Hayes, J. M.; Lyle, P. A.; Small, G. J. J. *Phys, Chem.* 1994, 98, 7337.

35. Rebane, K.K. Impurity spectra of solids. Plenum Press, 1970, New York.

36. Pieper, J; Freiberg, A. Electron – Phonon and exciton – phonon coupling in light harvesting, insights from line – narrowing spectroscopies. In review.

37. Oien, A. M.; Etelaars, M.; Kohler, J.; Aartsma, T. J.; Schmidt, J. *Science* 1999, 285, 400−402.

38.Tietz, C.; Cheklov, O.; Dr benstedt, A.; Schuster, J.; Wrachtrup, J. J. *Phys. Chem.* B 1999, 103, 6328.

39. Hofmann, C.; Michel, H.; van Heel, M.; Köhler, J. *Phys. Rev. Lett*. 2005, 94, 195501.

40. Brecht, M.; Studier, H.; Radics, V.; Nieder, J. B.; Bittl, R. J. *Am. Chem*. Soc. 2008, 130, 17487.

Non-exclusive licence to reproduce thesis and make thesis public

I, _____Galyna Gryliuk _____
(author's name)
(date of birth: _____17.11.1987_____),

1. herewith grant the University of Tartu a free permit (non-exclusive licence) to:

1.1. reproduce, for the purpose of preservation and making available to the public, including for addition to the DSpace digital archives until expiry of the term of validity of the copyright, and

1.2. make available to the public via the web environment of the University of Tartu, including via the DSpace digital archives until expiry of the term of validity of the copyright,

Electron- vibrational coupling in phycobiliproteins of Acaryochloris marina
_____,
(title of thesis)

_____Prof._ Jörg Pieper_____,
(supervisor's name)

2. I am aware of the fact that the author retains these rights.

3. I certify that granting the non-exclusive licence does not infringe the intellectual property rights or rights arising from the Personal Data Protection Act.

Tartu, __03.06.2013_____ (date)